

# THE UCSD/KECK DAMPED LY $\alpha$ ABUNDANCE DATABASE: A Decade of High Resolution Spectroscopy

Jason X. Prochaska<sup>1,2</sup>, Arthur M. Wolfe<sup>1,3</sup>, J. Christopher Howk<sup>1,4</sup>, Eric Gawiser<sup>1,5</sup>, Scott M. Burles<sup>1,6</sup>, Jeff Cooke<sup>1,7</sup>

## ABSTRACT

We publish the Keck/HIRES and Keck/ESI spectra that we have obtained during the first 10 years of Keck observatory operations. Our full sample includes 42 HIRES spectra and 39 ESI spectra along 65 unique sightlines providing abundance measurements on  $\approx 85$  DLA systems. The normalized data can be downloaded from the journal or from our supporting website: <http://www.ucolick.org/~xavier/DLA/>. The database includes all of the sightlines that have been included in our papers on the chemical abundances, kinematics, and metallicities of the damped Ly $\alpha$  systems. This data has also been used to argue for variations in the fine-structure constant. We present new chemical abundance measurements for 10 damped Ly $\alpha$  systems and a summary table of high-resolution metallicity measurements (including values from the literature) for 153 damped Ly $\alpha$  systems at  $z > 1.6$ . We caution, however, that this metallicity sample (and all previous ones) is biased to higher  $N_{\text{HI}}$  values than a random sample.

*Subject headings:* quasars : absorption lines, catalogs, ISM: abundances

<sup>1</sup>Visiting Astronomer, W.M. Keck Telescope. The Keck Observatory is a joint facility of the University of California, California Institute of Technology, and NASA.

<sup>2</sup>Department of Astronomy and Astrophysics, UCO/Lick Observatory; University of California, 1156 High Street, Santa Cruz, CA 95064; xavier@ucolick.org

<sup>3</sup>Department of Physics, and Center for Astrophysics and Space Sciences, University of California, San Diego, C-0424, La Jolla, CA 92093-0424

<sup>4</sup>Department of Physics, University of Notre Dame, Notre Dame, IN 46556

<sup>5</sup>NSF Astronomy and Astrophysics Postdoctoral Fellow, Yale Astronomy Department and Yale Center for Astronomy and Astrophysics, PO Box 208101, New Haven, CT 06520

<sup>6</sup>MIT Kavli Institute for Astrophysics and Space Research, Massachusetts Institute of Technology, 77 Massachusetts Avenue, Cambridge MA 02139

<sup>7</sup>Department of Physics and Astronomy and Center for Cosmology, University of California, Irvine, 4129 Frederick Reines Hall, Irvine, CA 92697-4575; cooke@uci.edu

## 1. Introduction

Since the discovery of the damped Ly $\alpha$  (DLA) systems (Wolfe *et al.* 1986), researchers have appreciated that high resolution spectra gives special insight into the interstellar medium (ISM) of high  $z$  galaxies in a fashion analogous with the local universe (e.g. Savage & Sembach 1996; Welty *et al.* 1999). For 8 years following this initial work, however, astronomers had access to only 4m-class telescopes and echelle observations were limited to the brightest quasars (e.g. D’Odorico & Savaglio 1991; Tripp, Lu & Savage 1996). The commissioning of the High Resolution Echelle Spectrometer (HIRES; Vogt *et al.* 1994) on the Keck I 10m telescope heralded a new era in the study of high  $z$  galaxies (Wolfe *et al.* 1994; Wolfe, Gawiser & Prochaska 2005). The years that followed witnessed the commissioning of additional echelle spectrometers on 10m-class telescopes – VLT/UVES (Dekker *et al.* 2000), Magellan/MIKE (Bernstein *et al.* 2003), Subaru/HDS (Noguchi *et al.* 2002) – and the commissioning of an echellette spectrometer on the Keck II 10m telescope (ESI Sheinis *et al.* 2002)). These technological advances have led to the research of many topics, including the kinematic characteristics (Prochaska & Wolfe 1997), metallicities (Prochaska & Wolfe 2000; Ledoux *et al.* 2006), depletion patterns (Lu *et al.* 1996; Pettini *et al.* 2000; Dessauges-Zavadsky *et al.* 2006), nucleosynthetic abundances (Lu *et al.* 1996; Molaro *et al.* 2000; Dessauges-Zavadsky *et al.* 2001), molecular fraction (Petitjean, Srianand & Ledoux 2000; Ledoux, Petitjean & Srianand 2003), and interstellar physics (Wolfe, Prochaska & Gawiser 2003; Howk, Wolfe & Prochaska 2005) for a sample of high redshift galaxies which are representative of the full galaxy distribution.

In this paper, we publish the spectra obtained by our group using the HIRES and ESI spectrometers during the first decade of Keck operations. Our full sample includes 42 HIRES spectra and 39 ESI spectra along 65 unique sightlines providing abundance measurements on 86 DLA systems. Previous papers have analyzed this data for many scientific purposes, and we refer the reader to those papers for further discussions: (1) gas kinematics (Prochaska & Wolfe 1997, 1998; Wolfe & Prochaska 1998, 2000; Prochaska & Wolfe 2001); (2) metallicity measurements (Prochaska & Wolfe 2000; Prochaska *et al.* 2003); (3) chemical abundances (Prochaska & Wolfe 1999, 2002; Prochaska, Howk & Wolfe 2003); (4) nitrogen enrichment (Prochaska *et al.* 2002); (5) photoionization (Prochaska *et al.* 2002); (6) star formation rates (Wolfe, Prochaska & Gawiser 2003; Wolfe, Gawiser & Prochaska 2003; Wolfe *et al.* 2004); (7) interstellar physics (Howk, Wolfe & Prochaska 2005); (8) variations of the fine-structure constant (Webb *et al.* 2001; Murphy *et al.* 2001); and (9) a survey of super-Lyman Limit systems (O’Meara *et al.* 2007).

Previously, the data has been proprietary and, unfortunately, current plans for the Keck

Observatory Archive (KOA<sup>1</sup>) do not include this dataset.<sup>2</sup> And, while we have mined these spectra extensively, we believe there are still new discoveries to be made. The ESI data, in particular, continue to offer new avenues of research, e.g., a molecular hydrogen survey (Milutinovich et al, in prep), studies of the Ly $\alpha$  forest (Abazajian et al., in prep), and an extensive survey for [C II] cooling rates (Wolfe et al., in prep). This paper and its associated on-line resources will make our full set of DLA observations freely available to the general astronomical community. The paper is summarized as follows. § 2 briefly describes the observations and data reduction procedures. § 3 presents Figures and Tables of previously unpublished (by our group) DLA transitions and abundance measurements. Finally, § 4 provides a brief summary.

## 2. SUMMARY OF OBSERVATIONS AND DATA REDUCTION

Most of the spectra presented here have been previously summarized in three papers (Prochaska & Wolfe 1999; Prochaska *et al.* 2001, 2003), but for completeness we provide a journal of all the observations in Tables 1 and 2, for HIRES and ESI respectively. For nearly all observations, the HIRES spectra were acquired using either a 0.8'' or 1.1'' wide decker ( $\text{FWHM} \approx 6$  and  $8 \text{ km s}^{-1}$ , respectively) and the ESI observations were carried out with the 0.5'' or 0.75'' slit ( $\text{FWHM} \approx 33$  and  $44 \text{ km s}^{-1}$ , respectively). All of the HIRES spectra were acquired with the original Tektronix 2048×2048 CCD. As such, we were reluctant to observe at wavelengths bluer than  $\lambda \approx 4000\text{\AA}$  or redward of  $\lambda \approx 8500\text{\AA}$ . In general we strove to achieve a final signal-to-noise (S/N) ratio of  $> 15$  per pixel ( $2 \text{ km s}^{-1} \text{ pix}^{-1}$  for HIRES,  $11 \text{ km s}^{-1} \text{ pix}^{-1}$  for ESI). ESI has a fixed format which covers the spectral region  $\lambda = 4000$  to  $10,000\text{\AA}$ .

With only two exceptions (Q1331+17, PHL957), all of the HIRES data were reduced with various versions of the MAKEE package,<sup>3</sup> kindly developed and distributed by T. Barlow. This data reduction pipeline bias subtracts and flattens the 2D images using standard techniques. It traces the object with the object itself, a standard star, or a pinhole spectrum of the quartz lamp. The data is sky-subtracted and optimally extracted. All but the original produced a 1D wavelength solution for each echelle order. The 1D spectra were coadded with various in-house algorithms that weighted by S/N ratio and rejected spuri-

---

<sup>1</sup><http://msc.caltech.edu/archives/koa/>

<sup>2</sup>Note that all HIRES data obtained by our group with the CCD mosaic (i.e. post September 2004) will be archived by KOA.

<sup>3</sup><http://spider.ipac.caltech.edu/staff/tbarlow/makee/>

ous pixels. In most cases, the data were first normalized using the *xplot* routine within MAKEE. This procedure was relatively straightforward because little of this HIRES data includes coverage the Ly $\alpha$  forest. The complete set of normalized, 1D spectra and error arrays are available with the electronic version of this paper and also at this online archive: <http://www.ucolick.org/~xavier/DLA/>. Note that the gaps in the spectra are echelle order gaps and occur redward of  $\approx 5200\text{\AA}$ .

All of the ESI observations were reduced with the ESIRedux package developed in IDL by J.X. Prochaska (Prochaska *et al.* 2003), which is publically available.<sup>4</sup> The majority of data were extracted with a simple boxcar aperture. Finally, the spectra are fluxed ( $\text{erg s}^{-1} \text{cm}^{-2} \text{\AA}^{-1}$ ) and fluxed with an archived sensitivity function. The flux is reasonably accurate ( $\approx 20\%$ ) in a relative sense but we have made no corrections for slit loss, airmass, or Galactic reddening. A continuum fit was derived for the data redward of the quasar Ly $\alpha$  emission feature using the *x\_continuum* routine within the XIDL package.<sup>5</sup> Both the fluxed and normalized spectra are available online. The spectra are continuous with the exception of the data near  $4500\text{\AA}$  where a chip blemish removes approx  $50\text{\AA}$  of data.

### 3. NEW ABUNDANCE MEASUREMENTS

Figures 1-10 present the HIRES observations for 10 of the damped Ly $\alpha$  systems that we had not previously published or had published only partially (e.g. FJ0812+32; Prochaska, Howk & Wolfe 2003). In each case, blends or bad spectral regions are indicated by dotted lines. The dashed vertical line at  $v = 0\text{km s}^{-1}$  corresponds to a somewhat arbitrary redshift (often corresponding to the peak optical depth in low-ion profiles) given in the figure captions. The dash-dot line indicates zero flux and the dashed line at unity traces the normalized quasar continuum.

We have derived ionic column densities from these data using primarily the apparent optical depth method (Savage & Sembach 1991). In a few cases (e.g. S II for the DLA at  $z = 2.626$  toward FJ0812+32), we have fitted Voigt profiles to the data using the VPFIT software package kindly provided by R. Carswell and J. Webb. In these cases, we adopt the total column density reported by the package. Otherwise we adopt the weighted-mean of the observed transitions or the most stringent upper/lower ( $2\sigma$ ) limit. All of the measurements are given in Tables 3-12. The errors only reflect statistical uncertainty using standard error propagation. These are unrealistic in the case of very high S/N (where  $\sigma \leq 0.01 \text{dex}$ ) or for

---

<sup>4</sup><http://www2.keck.hawaii.edu/inst/esi/ESIRedux/index.html>

<sup>5</sup><http://www.ucolick.org/~xavier/IDL/index.html>

very weak transitions where uncertainty in continuum placement dominates. We recommend a minimum error of 0.01 dex for strong transitions with high S/N data and 0.10 dex for weak transitions (peak optical depth less than 10%). See Prochaska *et al.* (2001) for a full description of our analysis procedures and a list of the atomic data, drawn primarily from Morton (2003).

In those cases where we have obtained both ESI and HIRES observations on a given sightline (e.g. Q1021+30, Q1209+09, Q1337+11, Q2342+34), we report the combined abundance measurements. With few exceptions, we give the HIRES observations precedence for the transitions where both datasets provide measurements. If our group had previously published column density measurements (e.g. Q1425+60; Prochaska *et al.* 2001), the full list is presented.

#### 4. DLA METAL SUMMARY

We now summarize the current set of high-resolution damped Ly $\alpha$  observations by listing all of the published metallicity measurements as of September 2006 (Table 13). We restrict the summary to optical data (i.e.  $z_{abs} > 1.6$ ) acquired at spectral resolution  $R > 5500$ , i.e. echelle or echellette observations. Although lower resolution observations can give accurate metal abundance measurements for favorable optical depth profiles (e.g. Pettini *et al.* 1994; Khare *et al.* 2004), we prefer to restrict the list to cases where the optical depth profile is at least partially resolved.

In general, the metallicities listed in Table 13 are [O/H], [Si/H], [S/H], or [Zn/H], in that order of preference. The elements O, S, and Zn have the advantage of being non-refractory and therefore the gas-phase abundances should reflect the total abundance. The difficulty with the latter element (Zn), however, is that it is a trace element (i.e. one expects 1 Zn atom per 10,000 O atoms) and it has an uncertain nucleosynthetic origin (Hoffman *et al.* 1996). It is difficult to measure O because its transitions are generally saturated while S often is lost within the Ly $\alpha$  forest or not covered by our observations. As such, Si is not frequently used for the metallicity.

Although Table 13 is a reasonably complete list of observed DLA systems, we emphasize that it should not be considered a representative sample of DLA systems. In particular, the  $N_{\text{HI}}$  frequency distribution of the sample does not follow that of a ‘random’ set of DLA systems. Figure 11 presents a histogram of the  $N_{\text{HI}}$  values for the metallicity sample given by Table 13. Overplotted on the histogram is the expected  $N_{\text{HI}}$  distribution for a random set of damped Ly $\alpha$  systems. This curve was generated from the  $N_{\text{HI}}$  frequency distribution

measured by Prochaska, Herbert-Fort & Wolfe (2005) from the Sloan Digital Sky Survey, Data Release 3 Abazajian *et al.* (2005). It is evident that the metallicity sample has too few DLA systems with  $N_{\text{HI}} < 10^{20.6} \text{ cm}^{-2}$ . A two-sided Kolmogorov-Smirnov test rules out the null hypothesis that the two distributions are drawn from the same parent population at  $> 99\%$ c.l.

We believe the difference shown in Figure 11 results primarily because observers (like ourselves) intentionally avoided low  $N_{\text{HI}}$  DLA systems when obtaining high resolution observations to be certain that their sample satisfied the  $N_{\text{HI}} \geq 2 \times 10^{20} \text{ cm}^{-2}$  criterion. Furthermore, we expect that some studies (e.g. H<sub>2</sub>; Ledoux, Petitjean & Srianand 2003) focused on large  $N_{\text{HI}}$  absorbers to increase their likelihood of detections. Because DLA metallicity is not strongly correlated with  $N_{\text{HI}}$  (Prochaska *et al.* 2003), the metallicity sample in Table 13 may not be significantly biased. Nevertheless, one must take care when drawing conclusions from this and other DLA datasets.

## 5. CONCLUDING REMARKS

In the future, our HIRES observations will be publically available via the Keck Observatory Archive. We also plan to release fully reduced, normalized 1D spectra in a fashion similar to this paper. We also plan to publish the next set of ESI spectra within the next two years.

The authors wish to recognize and acknowledge the very significant cultural role and reverence that the summit of Mauna Kea has always had within the indigenous Hawaiian community. We are most fortunate to have the opportunity to conduct observations from this mountain. JXP is partially supported by NSF grant AST 05-48180 and JXP and AMW acknowledge support from NSF grant AST 03-07408. This material is based upon work supported by the National Science Foundation under grant AST-0201667, an NSF Astronomy and Astrophysics Postdoctoral Fellowship (AAPF) awarded to E. Gawiser.

## REFERENCES

- Abazajian, K. *et al.* 2005, AJ, 129, 1755.  
Akerman, C. J. *et al.* 2005, A&A, 440, 499.

- Bernstein, R. *et al.* 2003, in Instrument Design and Performance for Optical/Infrared Ground-based Telescopes. Edited by Iye, Masanori; Moorwood, Alan F. M. Proceedings of the SPIE, Volume 4841, pp. 1694-1704 (2003)., 1694.
- Dekker, H. *et al.* 2000, in Proc. SPIE Vol. 4008, p. 534-545, Optical and IR Telescope Instrumentation and Detectors, Masanori Iye; Alan F. Moorwood; Eds., ed. M. Iye and A. F. Moorwood, 534.
- Dessauges-Zavadsky, M. *et al.* 2004, A&A, 416, 79.
- Dessauges-Zavadsky, M. *et al.* 2001, A&A, 370, 426.
- Dessauges-Zavadsky, M. *et al.* 2006, A&A, 445, 93.
- D'Odorico, S. and Savaglio, S. 1991, in Quasar Absorption Lines, ed. P. A. Shaver, E. J. Wampler, and A. M. Wolfe, 51.
- Ellison, S. L. *et al.* 2001, ApJ, 549, 770.
- Herbert-Fort, S. *et al.* 2006, PASP, 118, 1077.
- Hoffman, R. D. *et al.* 1996, ApJ, 460, 478.
- Howk, J. C., Wolfe, A. M., and Prochaska, J. X. 2005, ApJ, 622, L81.
- Khare, P. *et al.* 2004, ApJ, 616, 86.
- Ledoux, C. *et al.* 2006, A&A, 457, 71.
- Ledoux, C., Petitjean, P., and Srianand, R. 2003, MNRAS, 346, 209.
- Ledoux, C., Srianand, R., and Petitjean, P. 2002, A&A, 392, 781.
- Levshakov, S. A. *et al.* 2002, ApJ, 565, 696.
- Lopez, S. and Ellison, S. L. 2003, A&A, 403, 573.
- Lopez, S. *et al.* 2002, A&A, 385, 778.
- Lopez, S. *et al.* 1999, ApJ, 513, 598.
- Lu, L., Sargent, W. L. W., and Barlow, T. A. 1999, in ASP Conf. Ser. 156: Highly Redshifted Radio Lines, ed. C. L. Carilli, S. J. E. Radford, K. M. Menten, and G. I. Langston, 132.

- Lu, L. *et al.* 1996, ApJS, 107, 475.
- Molaro, P. *et al.* 2000, ApJ, 541, 54.
- Molaro, P. *et al.* 2001, ApJ, 549, 90.
- Morton, D. C. 2003, ApJS, 149, 205.
- Murphy, M. T. *et al.* 2001, MNRAS, 327, 1237.
- Noguchi, K. *et al.* 2002, PASJ, 54, 855.
- O'Meara, J. *et al.* 2007, ApJ, 622, in press (astro-ph/0610726).
- O'Meara, J. M. *et al.* 2006, ApJ, 649, L61.
- Petitjean, P., Srianand, R., and Ledoux, C. 2000, A&A, 364, L26.
- Pettini, M. *et al.* 2000, ApJ, 532, 65.
- Pettini, M. *et al.* 1994, ApJ, 426, 79.
- Prochaska, J. X., Castro, S., and Djorgovski, S. G. 2003, ApJS, 148, 317.
- Prochaska, J. X., Gawiser, E., and Wolfe, A. M. 2001, ApJ, 552, 99.
- Prochaska, J. X. *et al.* 2003a, ApJ, 595, L9.
- Prochaska, J. X. *et al.* 2003b, ApJS, 147, 227.
- Prochaska, J. X. *et al.* 2002a, PASP, 114, 933.
- Prochaska, J. X., Herbert-Fort, S., and Wolfe, A. M. 2005, ApJ, 635, 123.
- Prochaska, J. X. *et al.* 2002b, ApJ, 571, 693.
- Prochaska, J. X., Howk, J. C., and Wolfe, A. M. 2003, Nature, 423, 57.
- Prochaska, J. X. and Wolfe, A. M. 1996, ApJ, 470, 403.
- Prochaska, J. X. and Wolfe, A. M. 1997a, ApJ, 474, 140.
- Prochaska, J. X. and Wolfe, A. M. 1997b, ApJ, 487, 73.
- Prochaska, J. X. and Wolfe, A. M. 1998, ApJ, 507, 113.
- Prochaska, J. X. and Wolfe, A. M. 1999, ApJS, 121, 369.

- Prochaska, J. X. and Wolfe, A. M. 2000, ApJ, 533, L5.
- Prochaska, J. X. and Wolfe, A. M. 2001, ApJ, 560, L33.
- Prochaska, J. X. and Wolfe, A. M. 2002, ApJ, 566, 68.
- Prochaska, J. X. *et al.* 2001, ApJS, 137, 21.
- Savage, B. D. and Sembach, K. R. 1991, ApJ, 379, 245.
- Savage, B. D. and Sembach, K. R. 1996, ARA&A, 34, 279.
- Sheinis, A. I. *et al.* 2002, PASP, 114, 851.
- Songaila, A. and Cowie, L. L. 2002, AJ, 123, 2183.
- Tripp, T. M., Lu, L., and Savage, B. D. 1996, ApJS, 102, 239.
- Vogt, S. S. *et al.* 1994, in Proc. SPIE Instrumentation in Astronomy VIII, David L. Crawford; Eric R. Craine; Eds., Volume 2198, p. 362, 362.
- Webb, J. K. *et al.* 2001, Physical Review Letters, 87(9), 091301.
- Welty, D. E. *et al.* 1999, ApJ, 512, 636.
- Wolfe, A. M. *et al.* 1994, ApJ, 435, L101.
- Wolfe, A. M., Gawiser, E., and Prochaska, J. X. 2003, ApJ, 593, 235.
- Wolfe, A. M., Gawiser, E., and Prochaska, J. X. 2005, ARA&A, 43, 861.
- Wolfe, A. M. *et al.* 2004, ApJ, 615, 625.
- Wolfe, A. M. and Prochaska, J. X. 1998, ApJ, 494, L15+.
- Wolfe, A. M. and Prochaska, J. X. 2000, ApJ, 545, 591.
- Wolfe, A. M., Prochaska, J. X., and Gawiser, E. 2003, ApJ, 593, 215.
- Wolfe, A. M. *et al.* 1986, ApJS, 61, 249.

Table 1. JOURNAL OF HIRES OBSERVATIONS

QSO	Alt. Name	RA (J2000)	DEC (J2000)	Date (UT)	Exp (s)	Wavelengths (Å)	FWHM (km s <sup>-1</sup> )	S/N <sup>a</sup> (pix <sup>-1</sup> )	Conditions
Q0000–26		00:03:22.9	−26:03:17	30 Sep 1994	10800	6310–8130	8	15	
				01 Oct 1994	3600	6410–8130	8		
Q0019–15	BR 0019–1522	00:22:08.0	−15:05:39	20 Sep 1996	13500	5300–7800	8	18	Clouds
				21 Sep 1996	12600	5890–8320	6		Clouds
				22 Sep 1996	14400	5890–8320	8		Clouds
Q0100+13	PHL 957	01:03:11.4	+13:16:17	Spring 1994	11700	4420–6890	6	40	
Q0149+33	OC 383	01:52:34.4	+33:50:33	29 Sep 1997	8100	4080–6520	8	25	
				30 Sep 1997	9500	4080–6520	8		
				01 Oct 1997	6300	4080–6520	8		
Q0201+36	UT 0201+3634	02:04:55.6	+36:49:18	30 Sep 1994	11950	4720–7170	8	35	
				01 Oct 1994	13030	4720–7170	8		
Q0255+00	J0255+0048	02:55:18.6	+00:48:48	08 Nov 1999	9400	5800–8160	6	15	
				30 Nov 2000	10800	5800–8140	6		
Q0336–01		03:39:01.0	−01:33:18	01 Nov 2003	10800	4320–6750	6	15	
Q0347–38	...	03:49:43.5	−38:10:05	20 Sep 1996	4500	4890–7330	8	33	Clouds
				21 Sep 1996	1900	4890–7330	8		Thick Clouds
				22 Sep 1996	8100	4890–7330	8		Clouds
Q0458–02	PKS 0458–020	05:01:12.8	−01:59:14	31 Oct 1995	16200	3900–6290	8	15	
				01 Nov 1995	12600	3900–6290	8		
Q0741+47	HS0741+4741	07:45:21.8	+47:34:36	30 Nov 2000	5500	5050–7470	6	30	
Q0813+48	3C196	08:13:36	+48:13:03	08 Nov 1999	6600	3570–5975	8	10	
Q0812+32	FJ0812+32	08:12:40.8	+32:08:08	03 Mar 2002	10800	4330–6760	6	30	
				02 Nov 2002	9900	4330–6760	6		
Q0836+11		08:39:33.0	+11:12:04	26 Feb 1998	10800	4790–7180	8	17	
				11 Mar 2000	10100	4080–6510	8		
Q0841+12	...	08:44:24.3	+12:45:49	02 Nov 1997	7200	4810–7170	8	30	
				25 Feb 1998	7200	3900–6290	8		

Table 1—Continued

QSO	Alt. Name	RA (J2000)	DEC (J2000)	Date (UT)	Exp (s)	Wavelengths (Å)	FWHM (km s <sup>-1</sup> )	S/N <sup>a</sup> (pix <sup>-1</sup> )	Conditions
Q0900+42		09:00:32.9	+42:15:45	02 Mar 2002	7200	5140–7580	6	50	
				03 Mar 2002	7200	5140–7580	6		
Q0933+732		09:37:48.7	+73:01:58	12 Mar 2003	5400	4070–6500	6	15	
Q0948+43		09:48:35.7	+43:22:54	11 Mar 2003	5400	4010–6400	6	15	
Q0951–04	BR 0951–0450	09:53:55.7	−05:04:18	05 Apr 1997	14400	6030–8380	8	13	
				06 Apr 1997	16200	6030–8380	8		
Q0952–01	BRI 0952–0115	09:55:00.1	−01:30:07	19 Mar 1999	14400	5700–8150	8	15	
				20 Mar 1999	14400	5700–8150	8		Clouds
Q0957+33	PSS0957+33	09:57:44.5	+33:08:23	30 Nov 2000	7200	6440–8760	6	15	
Q1013-00		10:15:56.3	−00:35:05	25 Feb 1998	16200	6220–8550	8		
Q1013+00	BRI 1013+0035	10:15:49.0	+00:20:20	11 Mar 2000	10800	6140–8400	8	12	
				02 Mar 2002	5400	6220–8550	8		
Q1021+30		10:21:56.8	+30:01:31	02 Mar 2002	7200	4740–7170	6	15	
Q1108–07	BRI 1108–0747	11:11:13.6	−08:04:02	26 Feb 1998	14400	5950–8340	8	20	
				19 Mar 1999	7200	6000–8350	8		
				20 Mar 1999	5400	6000–8350	8		
Q1157+01		11:59:44.8	+01:12:07	02 Mar 2002	10800	3720–6090	6	30	
				03 Mar 2002	14200	3720–6090	6		
Q1209+09		12:11:34.1	+09:02:17	11 Mar 2003	5400	4080–6480	6	15	
				12 Mar 2003	5400	4080–6480	6		
Q1210+17		12:13:03.1	+17:14:23	12 Mar 2000	7200	3760–6170	8	20	
Q1215+33	GC 1215+3322	12:17:32.5	+33:05:38	Spring 1994	14040	3900–6300	8	20	
Q1223+17		12:26:07.2	+17:36:49	25 Feb 1998	10100	4780–7160	8	30	
				26 Feb 1998	9000	4780–7160	8		
Q1331+17	MC 1331+170	13:33:35.8	+16:49:04	Spring 1994	36000	4220–6625	6	80	
Q1337+11		13:40:02.4	+11:06:30	12 Mar 2000	8100	4650–7040	8	12	
Q1346–03	BRI 1346–0322	13:49:16.8	−03:37:15	05 Apr 1997	15900	5925–8340	8	29	

Table 1—Continued

QSO	Alt. Name	RA (J2000)	DEC (J2000)	Date (UT)	Exp (s)	Wavelengths (Å)	FWHM (km s <sup>-1</sup> )	S/N <sup>a</sup> (pix <sup>-1</sup> )	Conditions	
Q1425+60		14:26:56.4	+60:25:43	06 Apr 1997	14400	5925–8340	8	40		
				02 Mar 2002	2700	5620–7970	6			
Q1443+27	PSS1443+2724	14:43:31.2	+27:24:37	03 Mar 2002	1800	5620–7970	6	20	Clouds	
				19 Mar 1999	10800	6070–8500	8			
				20 Mar 1999	14400	6070–8500	8			
Q1759+75	GB1759+7539	17:57:46.4	+75:39:16	11 Mar 2000	11000	6070–8500	8	33	Clouds Clouds	
				21 Sep 1996	5044	5200–7570	6			
				22 Sep 1996	5400	5200–7570	6			
Q2206–19	...	22:08:52.0	−19:43:58	30 Sep 1994	7200	3940–6520	8	40		
				01 Oct 1994	7900	3940–6520	8			
Q2230+02	LBQS 2230+0232	22:32:35.3	+02:47:55	29 Sep 1997	7200	3890–6280	8	26		
				30 Sep 1997	5400	3890–6280	8			
				30 Sep 1997	5400	4430–6890	8			
				01 Oct 1997	9600	4430–6890	8			
				Fall 1995	14400	3990–6405	8			
Q2231–00	LBQS 2230–0015	22:34:08.8	+00:00:02					30		
Q2340–00	J234023–005327	23:40:23.7	−00:53:27	01 Nov 2003	3600	3920–6300	8	18		
Q2342+34		23:44:51.1	+34:33:47	01 Nov 2003	7200	4660–7100	8	12		
Q2348–01		23:50:57.8	−00:52:10	08 Nov 1999	10800	5060–7480	8	15		
				30 Nov 2000	5400	5060–7480	8			
				20 Sep 1996	4500	3860–6290	8		Poor seeing Clouds Clouds	
Q2348–14	...	23:51:29.9	−14:27:48	21 Sep 1996	5400	3860–6290	8			
				22 Sep 1996	3600	3860–6290	8			
				30 Sep 1997	10800	4110–6510	8	17		
Q2359–02	UM 196	00:01:50.0	−01:59:40	29 Sep 1997	14400	4110–6510	8			
				01 Oct 1997	12516	4110–6510	8			

<sup>a</sup>Total S/N ratio of the final spectrum at the central wavelength of the data.

Table 2. JOURNAL OF ESI OBSERVATIONS

QSO	RA (J2000)	DEC (J2000)	$z_{em}$	Date (UT)	FWHM (km s $^{-1}$ )	Exp (s)	S/N $^a$ (pix $^{-1}$ )
PX0034+16	00 34 54.8	+16 39 20	4.29	15 Oct 2001	33	4200	27
PSS0106+2601	01 06 00.8	+26 01 03	4.32	22 Jan 2001	44	1800	7
Q0112-30	01 15 04.8	-30 25 14	2.99	15 Oct 2001	33	2400	6
SDSS0127-00	01 27 00.7	-00 45 59	4.06	22 Jan 2001	44	1800	23
				19 Jul 2001	33	1800	
PSS0133+0400	01 33 40.4	+04 00 59	4.13	22 Jan 2001	44	1800	28
PSS0134+3317	01 34 21.6	+33 07 56	4.52	15 Oct 2001	33	6000	25
PSS0209+0517	02 09 44.7	+05 17 14	4.18	22 Jan 2001	44	1200	29
BRJ0426-2202	04 26 10.3	-22 02 17	4.30	22 Jan 2001	33	1800	25
FJ0747+2739	07 47 11.2	+27 39 04	4.11	15 Oct 2001	33	6000	31
PSS0808+5215	08 08 49.5	+52 15 16	4.45	07 Apr 2000	44	2400	28
FJ0812+32	08 12 40.8	+32 08 08	2.70	22 Jan 2001	33	1200	41
Q0821+31	08 21 07.6	+31 07 35	2.61	22 Jan 2001	33	1200	47
Q0930+28	09 33 37.8	+28 45 35	3.42	22 Jan 2001	33	1200	29
PC0953+4749	09 56 25.2	+47 34 44	4.46	22 Jan 2001	33	4800	10
PSS0957+3308	09 57 44.5	+33 08 24	4.25	07 Apr 2000	44	1200	30
BQ1021+3001	10 21 56.8	+30 01 31	3.12	22 Jan 2001	44	1800	26
CTQ460	10 39 09.4	-23 13 26	3.13	22 Jan 2001	33	1800	41
HS1132+2243	11 35 08.0	+22 27 07	2.88	22 Jan 2001	33	1200	33
BRI1144-0723	11 46 35.6	-07 40 05	4.16	07 Apr 2000	44	2400	40
PSS1159+1337	11 59 06.5	+13 37 38	4.07	22 Jan 2001	33	1200	26
Q1209+0919	12 11 34.1	+09 02 17	3.30	22 Jan 2001	33	1800	18
PSS1248+3110	12 48 20.2	+31 10 44	4.35	07 Apr 2000	44	2400	22
PSS1253-0228	12 53 36.3	-02 28 08	4.01	22 Jan 2001	33	2700	15
Q1337+11	13 40 02.4	+11 06 30	2.92	22 Jan 2001	33	2400	21
PKS1354-17	13 57 05.9	-17 44 06	3.15	19 Jul 2001	33	1800	8
PSS1432+3940	14 32 24.9	+39 40 24	4.28	07 Apr 2000	44	3600	15

Table 2—Continued

QSO	RA (J2000)	DEC (J2000)	$z_{em}$	Date (UT)	FWHM (km s $^{-1}$ )	Exp (s)	S/N $^a$ (pix $^{-1}$ )
HS1437+30	14 39 12.7	+29 54 41	2.99	22 Jan 2001	33	900	31
Q1502+4837	15 02 27.3	+48 37 09	3.20	19 Jul 2001	33	1800	10
PSS1506+5220	15 06 54.6	+52 20 05	4.18	22 Jan 2001	33	1200	27
PSS1723+2243	17 23 23.2	+22 43 58	4.52	19 Jul 2001	33	1800	36
FJ2129+00	21 29 16.7	+00 37 58	2.94	15 Oct 2001	33	900	25
PSS2155+1358	21 55 02.1	+13 58 26	4.26	31 Oct 2000	44	1800	30
Q2223+20	22 25 37.0	+20 40 18	3.56	15 Oct 2001	33	3000	35
PSS2241+1352	22 41 47.9	+13 52 03	4.44	19 Jul 2001	33	2700	18
PSS2323+2758	23 23 41.0	+27 58 01	4.18	19 Jul 2001	33	3600	18
FJ2334-09	23 34 46.4	-09 08 12	3.33	15 Oct 2001	33	2400	33
Q2342+34	23 44 51.1	+34 33 47	3.01	19 Jul 2001	33	1800	20
PSS2344+0342	23 44 03.2	+03 42 26	4.30	19 Jul 2001	33	1800	18
SDSS2350-00	23 50 58.2	-00 52 15	3.01	19 Jul 2001	33	2700	20

<sup>a</sup>Median signal-to-noise per 11km s $^{-1}$  pixel at  $\lambda \approx 7100\text{\AA}$ .

Note. — All of the observing nights were reasonably clear with seeing FWHM < 1''.

Table 3. IONIC COLUMN DENSITIES FOR FJ0812+32  $z = 2.0668$ 

Ion	$\lambda$ (Å)	$\log f$	Instr.	$v_{int}^a$ (km s $^{-1}$ )	$W_\lambda^b$ (mÅ)	$\log N$	$\log N_{adopt}$
C I							
	1560.3092	-0.8808	HIRES	[−15, 5]	7.7 ± 1.1	12.47 ± 0.06	12.60 ± 0.02
	1656.9283	-0.8273	HIRES	[−15, 2]	13.2 ± 0.8	12.64 ± 0.03	
C IV							
	1548.1950	-0.7194	HIRES	[−100, 100]	252.0 ± 2.6	13.95 ± 0.01	13.95 ± 0.01
	1550.7700	-1.0213	HIRES	[−100, 100]	148.0 ± 2.9	13.95 ± 0.01	
Al II							
	1670.7874	0.2742	HIRES	[−80, 40]	220.0 ± 2.2	> 13.13	> 13.13
Al III							
	1854.7164	-0.2684	HIRES	[−30, 50]	27.4 ± 1.5	12.25 ± 0.02	12.25 ± 0.02
	1862.7895	-0.5719	HIRES	[−30, 50]	15.2 ± 1.5	12.28 ± 0.04	
Si II							
	1526.7066	-0.8962	HIRES	[−100, 30]	224.5 ± 2.4	> 14.47	15.18 ± 0.01
	1808.0130	-2.6603	HIRES	[−30, 20]	64.0 ± 1.4	15.18 ± 0.01	
Ti II							
	1910.6000	-0.9830	HIRES	[−10, 20]	10.8 ± 0.9	12.54 ± 0.04	12.53 ± 0.03
	1910.9380	-1.0088	HIRES	[−15, 10]	10.1 ± 0.8	12.53 ± 0.04	
Cr II							
	2056.2539	-0.9788	HIRES	[−20, 20]	47.4 ± 4.0	13.20 ± 0.04	13.24 ± 0.01
	2062.2340	-1.1079	HIRES	[−20, 20]	41.2 ± 1.3	13.24 ± 0.01	
	2066.1610	-1.2882	HIRES	[−20, 20]	30.2 ± 1.3	13.26 ± 0.02	
Mn II							
	2594.4990	-0.5670	HIRES	[−20, 20]	58.7 ± 4.9	12.65 ± 0.04	12.65 ± 0.03
	2606.4620	-0.7151	HIRES	[−20, 20]	43.3 ± 6.2	12.63 ± 0.06	
Fe II							
	1608.4511	-1.2366	HIRES	[−50, 30]	145.3 ± 1.7	> 14.48	14.89 ± 0.02
	1611.2005	-2.8665	HIRES	[−15, 15]	21.1 ± 1.1	14.89 ± 0.02	
Co II							
	1941.2852	-1.4685	HIRES	[−10, 10]	< 1.5	< 12.31	< 12.31
Ni II							
	1454.8420	-1.4908	HIRES	[−20, 20]	20.7 ± 1.5	13.59 ± 0.03	13.62 ± 0.01
	1467.2590	-2.2007	HIRES	[−10, 10]	4.0 ± 0.7	13.54 ± 0.08	
	1467.7560	-2.0044	HIRES	[−10, 10]	6.2 ± 0.7	13.53 ± 0.05	
	1703.4050	-2.2218	HIRES	[−20, 20]	6.7 ± 1.2	13.65 ± 0.08	
	1741.5531	-1.3696	HIRES	[−30, 10]	40.7 ± 1.2	13.64 ± 0.01	
	1751.9157	-1.5575	HIRES	[−20, 10]	26.9 ± 1.2	13.62 ± 0.02	

Table 3—Continued

Ion	$\lambda$ (Å)	$\log f$	Instr.	$v_{int}^a$ (km s $^{-1}$ )	$W_\lambda^b$ (mÅ)	$\log N$	$\log N_{adopt}$
Zn II							
	2026.1360	−0.3107	HIRES	[−15, 15]	$27.1 \pm 1.1$	$12.24 \pm 0.02$	$12.21 \pm 0.02$
	2062.6640	−0.5918	HIRES	[−20, 20]	$10.9 \pm 1.3$	$12.09 \pm 0.05$	
Ga II							
	1414.4020	0.2553	HIRES	[−10, 10]	$9.2 \pm 2.4$	< 11.50	< 11.50
Ge II							
	1602.4863	−0.8428	HIRES	[−10, 10]	< 2.0	< 11.98	< 11.98

<sup>a</sup>Velocity interval over which the equivalent width and column density are measured.

<sup>b</sup>Rest equivalent width.

Table 4. IONIC COLUMN DENSITIES FOR FJ0812+32  $z = 2.6263$ 

Ion	$\lambda$ (Å)	$\log f$	Instr.	$v_{int}^a$ (km s $^{-1}$ )	$W_\lambda^b$ (mÅ)	$\log N$	$\log N_{adopt}$
B II							
C I	1362.4610	-0.0057	HIRES	[−15, 15]	$4.3 \pm 0.9$	$11.43 \pm 0.09$	$11.43 \pm 0.09$
C II	1328.8333	-1.0467	HIRES	[−20, 20]	$10.5 \pm 1.1$	$12.90 \pm 0.04$	$12.75 \pm 0.03$
	1560.3092	-0.8808	HIRES	[−20, 20]	$13.7 \pm 1.0$	$12.71 \pm 0.03$	
	1656.9283	-0.8273	HIRES	[−20, 20]	$19.4 \pm 1.1$	$> 12.77$	
C IV	1334.5323	-0.8935	HIRES	[−110, 70]	$641.1 \pm 1.7$	$> 15.20$	$> 15.20$
	1335.7077	-0.9397	HIRES	[−50, 70]	$129.9 \pm 1.7$	$14.03 \pm 0.01$	
N I	1548.1950	-0.7194	HIRES	[−140, 300]	$860.7 \pm 4.1$	$> 14.61$	$14.59 \pm 0.01$
O I	1550.7700	-1.0213	HIRES	[−140, 300]	$571.7 \pm 3.2$	$14.59 \pm 0.01$	
Mg II	1200.7098	-1.3665	HIRES	[−20, 30]	$162.2 \pm 1.8$	$> 15.04$	$16.00 \pm 0.34$
Al II	1302.1685	-1.3110	HIRES	[−100, 80]	$567.4 \pm 2.5$	$> 15.56$	$17.49 \pm 0.09$
Al III	1239.9253	-3.1986	HIRES	[−50, 50]	$122.0 \pm 1.2$	$16.29 \pm 0.01$	$16.24 \pm 0.01$
	1355.5977	-5.9066	HIRES	[−20, 20]	$6.0 \pm 1.3$	$17.49 \pm 0.09$	
Si II	1240.3947	-3.4498	HIRES	[−50, 40]	$55.6 \pm 1.2$	$16.14 \pm 0.01$	
Si IV	1670.7874	0.2742	HIRES	[−160, 100]	$662.7 \pm 1.9$	$> 13.80$	$> 13.80$
	1854.7164	-0.2684	HIRES	[−100, 100]	$217.6 \pm 2.0$	$13.28 \pm 0.01$	$13.28 \pm 0.01$
S II	1862.7895	-0.5719	HIRES	[−100, 100]	$124.4 \pm 2.3$	$13.27 \pm 0.01$	
	1260.4221	0.0030	HIRES	[−110, 60]	$639.4 \pm 1.3$	$> 14.36$	$15.98 \pm 0.05$
	1304.3702	-1.0269	HIRES	[−100, 80]	$462.2 \pm 2.2$	$> 15.14$	
	1526.7066	-0.8962	HIRES	[−120, 80]	$599.5 \pm 2.0$	$> 15.01$	
	1808.0130	-2.6603	HIRES	[−80, 40]	$245.8 \pm 1.9$	$> 15.98$	
	1393.7550	-0.2774	HIRES	[−150, 260]	$701.6 \pm 3.7$	$14.09 \pm 0.01$	$14.07 \pm 0.01$
	1402.7700	-0.5817	HIRES	[−130, 250]	$401.9 \pm 2.9$	$14.06 \pm 0.01$	
	1250.5840	-2.2634	HIRES	[−70, 40]	$154.9 \pm 1.5$	$> 15.62$	$15.63 \pm 0.08$
	1253.8110	-1.9634	HIRES	[−70, 60]	$202.6 \pm 2.0$	$> 15.57$	

Table 4—Continued

Ion	$\lambda$ (Å)	$\log f$	Instr.	$v_{int}^a$ (km s $^{-1}$ )	$W_\lambda^b$ (mÅ)	$\log N$	$\log N_{adopt}$
Cl I	1259.5190	−1.7894	HIRES	[−100, 60]	$249.9 \pm 1.8$	$> 15.52$	
	1347.2400	−0.9259	HIRES	[−30, 20]	$16.7 \pm 1.1$	$12.98 \pm 0.03$	$12.98 \pm 0.03$
Ti II	1910.6000	−0.9830	HIRES	[−20, 35]	$21.8 \pm 4.7$	$12.84 \pm 0.09$	$12.90 \pm 0.06$
	1910.9380	−1.0088	HIRES	[−20, 35]	$26.0 \pm 4.6$	$12.95 \pm 0.08$	
Cr II	2056.2539	−0.9788	HIRES	[−70, 30]	$78.6 \pm 5.1$	$13.36 \pm 0.03$	$13.36 \pm 0.03$
	2066.1610	−1.2882	HIRES	[−70, 30]	$57.1 \pm 6.1$	$< 13.52$	
Mn II	1197.1840	−0.8052	HIRES	[−20, 30]	$18.7 \pm 2.1$	$< 13.00$	$< 13.00$
Fe II	1608.4511	−1.2366	HIRES	[−100, 80]	$405.2 \pm 1.7$	$> 14.97$	$15.09 \pm 0.01$
	1611.2005	−2.8665	HIRES	[−50, 20]	$35.3 \pm 1.1$	$15.09 \pm 0.01$	
	2249.8768	−2.7397	HIRES	[−70, 30]	$100.1 \pm 8.1$	$15.15 \pm 0.04$	
Co II	1466.2120	−1.5086	HIRES	[−15, 15]	$< 1.9$	$< 12.68$	$< 12.68$
	2012.1664	−1.4343	HIRES	[−50, 50]	$16.1 \pm 5.2$	$< 13.13$	
Ni II	1317.2170	−1.2434	HIRES	[−80, 50]	$65.2 \pm 2.1$	$13.93 \pm 0.01$	$13.89 \pm 0.01$
	1370.1310	−1.2306	HIRES	[−80, 40]	$70.3 \pm 1.7$	$13.92 \pm 0.01$	
	1454.8420	−1.4908	HIRES	[−50, 20]	$30.8 \pm 2.3$	$13.74 \pm 0.03$	
	1467.2590	−2.2007	HIRES	[−20, 20]	$6.2 \pm 1.0$	$13.72 \pm 0.07$	
	1467.7560	−2.0044	HIRES	[−20, 20]	$10.0 \pm 1.0$	$13.74 \pm 0.04$	
	1703.4050	−2.2218	HIRES	[−20, 20]	$6.6 \pm 1.0$	$13.64 \pm 0.07$	
	1741.5531	−1.3696	HIRES	[−60, 30]	$79.2 \pm 2.3$	$13.91 \pm 0.01$	
	1751.9157	−1.5575	HIRES	[−50, 30]	$51.0 \pm 1.4$	$13.87 \pm 0.01$	
Zn II	2026.1360	−0.3107	HIRES	[−70, 30]	$162.8 \pm 6.3$	$13.15 \pm 0.02$	$13.15 \pm 0.02$
Ga II	1414.4020	0.2553	HIRES	[−10, 10]	$< 1.9$	$< 10.95$	$< 10.95$
Ge II	1237.0590	0.0888	HIRES	[−50, 20]	$15.6 \pm 1.3$	$12.00 \pm 0.04$	$12.01 \pm 0.04$
	1602.4863	−0.8428	HIRES	[−20, 20]	$4.4 \pm 1.0$	$12.13 \pm 0.10$	

<sup>a</sup>Velocity interval over which the equivalent width and column density are measured.

<sup>b</sup>Rest equivalent width.

Table 5. IONIC COLUMN DENSITIES FOR J0900+42  $z = 3.2458$

Ion	$\lambda$ (Å)	$\log f$	Instr.	$v_{int}^a$ (km s $^{-1}$ )	$W_\lambda^b$ (mÅ)	$\log N$	$\log N_{adopt}$
C I							
	1328.8333	−1.0467	HIRES	[−20, 20]	< 1.4	< 12.18	11.79 ± 0.14
	1560.3092	−0.8808	HIRES	[−20, 20]	< 1.1	< 11.75	
	1656.9283	−0.8273	HIRES	[−5, 20]	2.2 ± 0.7	11.79 ± 0.14	
C II							
	1334.5323	−0.8935	HIRES	[−100, 100]	624.6 ± 1.1	> 15.23	> 15.23
	1335.7077	−0.9397	HIRES	[−70, 20]	15.0 ± 1.0	12.93 ± 0.03	
C IV							
	1548.1950	−0.7194	HIRES	[−140, 90]	141.5 ± 1.5	13.60 ± 0.01	13.60 ± 0.01
N V							
	1238.8210	−0.8041	HIRES	[−25, 10]	< 0.8	< 11.72	< 11.72
Mg II							
	1239.9253	−3.1986	HIRES	[−30, 30]	3.9 ± 0.5	14.67 ± 0.06	14.64 ± 0.05
	1240.3947	−3.4498	HIRES	[−30, 30]	1.7 ± 0.5	14.56 ± 0.13	
Al II							
	1670.7874	0.2742	HIRES	[−100, 100]	566.8 ± 1.6	> 13.59	> 13.59
Si II							
	1304.3702	−1.0269	HIRES	[−100, 100]	419.9 ± 1.4	> 14.95	> 14.95
Si IV							
	1393.7550	−0.2774	HIRES	[−100, 90]	178.6 ± 1.6	13.44 ± 0.01	13.44 ± 0.01
	1402.7700	−0.5817	HIRES	[−100, 90]	103.2 ± 1.3	13.44 ± 0.01	
S II							
	1250.5840	−2.2634	HIRES	[−80, 60]	31.4 ± 0.8	14.64 ± 0.01	14.65 ± 0.01
	1259.5190	−1.7894	HIRES	[−80, 60]	88.3 ± 0.9	14.65 ± 0.01	
Fe II							
	1608.4511	−1.2366	HIRES	[−100, 80]	295.3 ± 1.7	14.54 ± 0.01	14.54 ± 0.01
	1611.2005	−2.8665	HIRES	[−90, 70]	6.8 ± 1.7	14.35 ± 0.11	
Ni II							
	1370.1310	−1.2306	HIRES	[−50, 30]	20.1 ± 1.1	13.33 ± 0.02	13.30 ± 0.02
	1454.8420	−1.4908	HIRES	[−50, 20]	8.8 ± 1.1	13.17 ± 0.05	
	1741.5531	−1.3696	HIRES	[−50, 30]	22.7 ± 1.6	13.32 ± 0.03	
	1751.9157	−1.5575	HIRES	[−50, 30]	13.5 ± 1.4	13.27 ± 0.04	

<sup>a</sup>Velocity interval over which the equivalent width and column density are measured.

<sup>b</sup>Rest equivalent width.

Table 6. IONIC COLUMN DENSITIES FOR B1013+0035  $z = 3.1040$

Ion	$\lambda$ (Å)	$\log f$	Instr.	$v_{int}^a$ (km s $^{-1}$ )	$W_\lambda^b$ (mÅ)	$\log N$	$\log N_{adopt}$
C IV							
	1548.1950	−0.7194	HIRES	[−100, 200]	$1068.2 \pm 7.1$	$> 14.77$	$> 14.77$
Al II	1670.7874	0.2742	HIRES	[−100, 240]	$1592.6 \pm 8.4$	$> 14.07$	$> 14.07$
Si II	1808.0130	−2.6603	HIRES	[−90, 230]	$295.6 \pm 10.5$	$15.78 \pm 0.02$	$15.78 \pm 0.02$
Cr II	2056.2539	−0.9788	HIRES	[0, 100]	$54.5 \pm 10.7$	$> 13.21$	$> 13.21$
	2066.1610	−1.2882	HIRES	[−80, 120]	$< 29.6$	$< 13.45$	
Fe II	1608.4511	−1.2366	HIRES	[−100, 240]	$883.1 \pm 4.0$	$> 15.15$	$15.18 \pm 0.05$
	1611.2005	−2.8665	HIRES	[−100, 240]	$43.1 \pm 5.1$	$15.18 \pm 0.05$	
Ni II	1741.5531	−1.3696	HIRES	[−80, 200]	$71.8 \pm 10.1$	$13.89 \pm 0.05$	$13.89 \pm 0.05$
Zn II	2026.1360	−0.3107	HIRES	[−80, 240]	$298.4 \pm 12.7$	$13.33 \pm 0.02$	$13.33 \pm 0.02$

<sup>a</sup>Velocity interval over which the equivalent width and column density are measured.

<sup>b</sup>Rest equivalent width.

Table 7. IONIC COLUMN DENSITIES FOR Q1021+30  $z = 2.9489$

Ion	$\lambda$ (Å)	$\log f$	Instr.	$v_{int}^a$ (km s $^{-1}$ )	$W_\lambda^b$ (mÅ)	$\log N$	$\log N_{adopt}$
C I							
	1560.3092	−0.8808	HIRES	[−40, 60]	$13.7 \pm 4.2$	< 12.71	< 12.71
	1656.9283	−0.8273	ESI	[−50, 50]	< 15.5	< 12.81	
C II							
	1334.5323	−0.8935	HIRES	[−100, 150]	$467.5 \pm 6.4$	> 14.77	> 14.77
	1335.7077	−0.9397	HIRES	[−15, 50]	< 7.8	< 12.81	
C IV							
	1548.1950	−0.7194	HIRES	[−100, 150]	$316.3 \pm 7.1$	$14.01 \pm 0.01$	$13.99 \pm 0.01$
	1550.7700	−1.0213	HIRES	[−100, 150]	$157.0 \pm 7.1$	$13.95 \pm 0.02$	
N I							
	1200.2233	−1.0645	HIRES	[0, 50]	< 7.0	> 13.03	$13.41 \pm 0.09$
	1200.7098	−1.3665	HIRES	[−30, 2]	$13.1 \pm 2.8$	$13.41 \pm 0.09$	
O I							
	1302.1685	−1.3110	HIRES	[−70, 130]	$311.2 \pm 3.8$	> 15.09	> 15.09
Mg II							
	1239.9253	−3.1986	HIRES	[−50, 50]	$18.3 \pm 3.4$	< 15.36	< 15.35
Al III							
	1854.7164	−0.2684	ESI	[−80, 100]	< 27.2	< 12.40	< 12.40
Si II							
	1304.3702	−1.0269	HIRES	[−70, 130]	$168.4 \pm 4.0$	$14.32 \pm 0.02$	$14.32 \pm 0.02$
	1526.7066	−0.8962	HIRES	[−70, 140]	$250.5 \pm 6.6$	> 14.35	
	1808.0126	−2.6603	HIRES	[−60, 80]	< 36.2	< 14.47	
Si IV							
	1393.7550	−0.2774	HIRES	[−100, 150]	$263.0 \pm 6.5$	$13.60 \pm 0.01$	$13.62 \pm 0.01$
	1402.7700	−0.5817	HIRES	[−100, 150]	$177.3 \pm 7.2$	$13.66 \pm 0.02$	
S II							
	1253.8110	−1.9634	HIRES	[−40, 20]	$10.6 \pm 1.8$	$13.87 \pm 0.07$	$13.87 \pm 0.07$
Cr II							
	2056.2539	−0.9788	ESI	[−40, 60]	< 19.6	< 12.89	< 12.89
Fe II							
	1121.9748	−1.6946	ESI	[−50, 50]	$34.3 \pm 7.9$	$14.22 \pm 0.10$	$14.04 \pm 0.01$
	1608.4511	−1.2366	HIRES	[−70, 100]	$110.2 \pm 3.6$	$14.04 \pm 0.01$	
	1611.2005	−2.8665	HIRES	[−40, 70]	< 5.3	< 14.41	
	2344.2140	−0.9431	ESI	[−60, 60]	$200.0 \pm 15.3$	> 13.65	
Ni II							
	1317.2170	−1.2434	HIRES	[−40, 40]	< 7.6	< 13.12	< 13.04

Table 7—Continued

Ion	$\lambda$ (Å)	$\log f$	Instr.	$v_{int}^a$ (km s $^{-1}$ )	$W_\lambda^b$ (mÅ)	$\log N$	$\log N_{adopt}$
	1370.1310	−1.2306	HIRES	[−30, 50]	< 26.8	< 13.04	
	1454.8420	−1.4908	HIRES	[−40, 50]	< 7.5	< 13.26	
	1709.6042	−1.4895	HIRES	[−60, 80]	< 10.6	< 13.28	
Zn II							
	2026.1360	−0.3107	ESI	[−40, 80]	< 19.9	< 12.23	< 12.23

<sup>a</sup>Velocity interval over which the equivalent width and column density are measured.

<sup>b</sup>Rest equivalent width.

Table 8. IONIC COLUMN DENSITIES FOR Q1209+0919  $z = 2.5841$

Ion	$\lambda$ (Å)	$\log f$	Instr.	$v_{int}^a$ (km s $^{-1}$ )	$W_\lambda^b$ (mÅ)	$\log N$	$\log N_{adopt}$
C I							
	1560.3092	−0.8808	HIRES	[−50, 50]	< 8.8	< 12.67	12.60 ± 0.13
	1656.9283	−0.8273	HIRES	[−60, 60]	< 8.6	12.60 ± 0.13	
C IV							
	1548.1950	−0.7194	HIRES	[−300, 300]	1670.4 ± 10.4	> 14.97	> 15.02
	1550.7700	−1.0213	HIRES	[−240, 300]	1189.4 ± 9.4	> 15.02	
Al II							
	1670.7874	0.2742	ESI	[−300, 300]	1902.7 ± 23.6	> 14.07	> 14.07
Al III							
	1854.7164	−0.2684	ESI	[−200, 200]	640.9 ± 17.0	13.71 ± 0.01	13.74 ± 0.01
	1862.7895	−0.5719	ESI	[−200, 200]	473.8 ± 17.9	13.83 ± 0.02	
Si II							
	1526.7066	−0.8962	HIRES	[−300, 300]	1668.6 ± 9.7	> 15.34	15.91 ± 0.01
	1808.0126	−2.6603	HIRES	[−100, 200]	384.7 ± 6.9	15.91 ± 0.01	
Ti II							
	1910.6000	−0.9830	ESI	[−50, 50]	< 21.6	< 13.00	< 13.00
Cr II							
	2056.2539	−0.9788	ESI	[−100, 50]	145.7 ± 18.1	13.62 ± 0.06	13.61 ± 0.05
	2066.1610	−1.2882	ESI	[−50, 50]	67.2 ± 18.2	13.57 ± 0.12	
Mn II							
	2576.8770	−0.4549	ESI	[−100, 120]	257.9 ± 34.3	13.15 ± 0.06	13.16 ± 0.05
	2594.4990	−0.5670	ESI	[−100, 100]	219.4 ± 41.0	13.19 ± 0.08	
Fe II							
	1608.4511	−1.2366	HIRES	[−150, 210]	1046.9 ± 7.3	> 15.32	15.25 ± 0.03
	1611.2005	−2.8665	HIRES	[−80, 100]	53.4 ± 6.1	15.28 ± 0.05	
	2249.8768	−2.7397	ESI	[−70, 60]	147.9 ± 19.1	< 15.30	
	2260.7805	−2.6126	ESI	[−100, 80]	164.1 ± 17.2	15.22 ± 0.05	
	2344.2140	−0.9431	ESI	[−120, 200]	1861.2 ± 43.1	> 14.90	
	2374.4612	−1.5045	ESI	[−200, 250]	1369.7 ± 36.2	> 15.33	
	2382.7650	−0.4949	ESI	[−300, 300]	2658.3 ± 32.1	> 14.73	
Co II							
	2012.1665	−1.4343	ESI	[−50, 50]	< 27.2	< 13.52	< 13.52
Ni II							
	1454.8420	−1.4908	ESI	[−50, 50]	61.4 ± 5.6	14.04 ± 0.04	14.11 ± 0.02
	1703.4050	−2.2218	ESI	[−100, 100]	< 33.3	< 14.53	
	1741.5531	−1.3696	HIRES	[−30, 100]	127.2 ± 5.3	14.12 ± 0.02	

Table 8—Continued

Ion	$\lambda$ (Å)	$\log f$	Instr.	$v_{int}^a$ (km s $^{-1}$ )	$W_\lambda^b$ (mÅ)	$\log N$	$\log N_{adopt}$
Zn II	1751.9157	-1.5575	HIRES	[−100, 150]	$173.6 \pm 7.7$	< 14.41	
	2026.1360	-0.3107	ESI	[−100, 100]	$156.7 \pm 19.3$	$12.99 \pm 0.06$	$12.98 \pm 0.05$

<sup>a</sup>Velocity interval over which the equivalent width and column density are measured.

<sup>b</sup>Rest equivalent width.

Table 9. IONIC COLUMN DENSITIES FOR Q1337+11  $z = 2.79585$

Ion	$\lambda$ (Å)	$\log f$	Instr.	$v_{int}^a$ (km s $^{-1}$ )	$W_\lambda^b$ (mÅ)	$\log N$	$\log N_{adopt}$
C I	1560.3092	-0.8808	HIRES	[−60, 60]	< 12.0	< 12.81	< 12.66
	1656.9284	-0.8273	HIRES	[−40, 40]	< 10.8	< 12.66	
C II	1334.5323	-0.8935	HIRES	[−70, 50]	$282.0 \pm 6.1$	$> 14.64$	$> 14.64$
	1335.7077	-0.9397	HIRES	[−20, 40]	$29.8 \pm 4.4$	$13.28 \pm 0.06$	
C IV	1548.1950	-0.7194	HIRES	[−100, 30]	$81.3 \pm 6.0$	$13.36 \pm 0.03$	$13.39 \pm 0.03$
	1550.7700	-1.0213	HIRES	[−100, 30]	$60.4 \pm 6.8$	$13.52 \pm 0.05$	
N I	1199.5496	-0.8861	ESI	[−30, 40]	$109.3 \pm 9.7$	$13.94 \pm 0.05$	$13.94 \pm 0.05$
N V	1238.8210	-0.8041	HIRES	[−40, 40]	$10.1 \pm 3.0$	< 12.71	< 12.71
O I	1302.1685	-1.3110	HIRES	[−60, 80]	$254.0 \pm 4.7$	$> 15.09$	$> 15.09$
Al II	1670.7874	0.2742	HIRES	[−60, 40]	$216.3 \pm 4.9$	$> 13.03$	$> 13.03$
Al III	1854.7164	-0.2684	HIRES	[−50, 50]	$23.5 \pm 7.0$	$12.22 \pm 0.12$	$12.22 \pm 0.12$
	1862.7895	-0.5719	ESI	[−50, 50]	< 19.7	< 12.56	
Si II	1260.4221	0.0030	HIRES	[−60, 50]	$265.9 \pm 2.3$	$> 13.86$	$14.79 \pm 0.07$
	1304.3702	-1.0269	HIRES	[−50, 50]	$180.9 \pm 4.0$	$> 14.49$	
	1526.7066	-0.8962	ESI	[−80, 80]	$251.2 \pm 10.4$	$> 14.21$	
	1808.0130	-2.6603	HIRES	[−60, 30]	$35.5 \pm 5.5$	$14.79 \pm 0.07$	
Si IV	1393.7550	-0.2774	ESI	[−100, 20]	$75.4 \pm 10.2$	$12.97 \pm 0.06$	$12.93 \pm 0.05$
	1402.7700	-0.5817	HIRES	[−80, 20]	$31.1 \pm 5.3$	$12.89 \pm 0.07$	
S II	1259.5190	-1.7894	HIRES	[−40, 40]	$39.3 \pm 2.1$	$14.33 \pm 0.02$	$14.33 \pm 0.02$
Cr II	2056.2539	-0.9788	ESI	[−60, 60]	< 22.6	< 12.95	< 12.95
Mn II	2576.8770	-0.4549	ESI	[−50, 50]	< 51.8	< 12.58	< 12.58
Fe II	1608.4511	-1.2366	ESI	[−70, 70]	$118.5 \pm 6.4$	$14.06 \pm 0.02$	$14.07 \pm 0.02$

Table 9—Continued

Ion	$\lambda$ (Å)	$\log f$	Instr.	$v_{int}^a$ (km s $^{-1}$ )	$W_\lambda^b$ (mÅ)	$\log N$	$\log N_{adopt}$
	1611.2005	−2.8665	HIRES	[−40, 40]	< 7.9	< 14.59	
	2260.7805	−2.6126	ESI	[−50, 50]	< 24.4	< 14.54	
	2344.2140	−0.9431	ESI	[−80, 80]	$295.3 \pm 15.3$	> 13.90	
	2374.4612	−1.5045	ESI	[−80, 80]	$177.8 \pm 15.1$	$14.13 \pm 0.04$	
	2382.7650	−0.4949	ESI	[−80, 80]	$383.7 \pm 15.7$	> 13.63	
	2586.6500	−1.1605	ESI	[−80, 80]	$344.2 \pm 36.9$	$14.01 \pm 0.05$	
	2600.1729	−0.6216	ESI	[−80, 80]	$376.6 \pm 35.0$	> 13.59	
Ni II							
	1317.2170	−1.2434	HIRES	[−40, 40]	< 10.2	< 13.26	$13.27 \pm 0.08$
	1370.1310	−1.2306	HIRES	[−40, 30]	$19.9 \pm 5.3$	$13.36 \pm 0.11$	
	1741.5531	−1.3696	HIRES	[−40, 40]	$16.7 \pm 4.9$	$13.21 \pm 0.12$	
Zn II							
	2026.1360	−0.3107	ESI	[−50, 50]	< 20.6	< 12.25	< 12.25

<sup>a</sup>Velocity interval over which the equivalent width and column density are measured.

<sup>b</sup>Rest equivalent width.

Table 10. IONIC COLUMN DENSITIES FOR Q1425+60  $z = 2.8268$

Ion	$\lambda$ (Å)	$\log f$	Instr.	$v_{int}^a$ (km s $^{-1}$ )	$W_\lambda^b$ (mÅ)	$\log N$	$\log N_{adopt}$
C I							
	1560.3092	−0.8808	ESI	[−80, 60]	< 4.6	< 12.39	< 12.39
C II							
	1036.3367	−0.9097	HIRES	[−120, 120]	$680.2 \pm 18.4$	> 15.22	> 15.23
	1335.7077	−0.9397	HIRES	[−20, 20]	$43.4 \pm 0.8$	< 13.52	
C IV							
	1548.1950	−0.7194	ESI	[−150, 350]	$1108.0 \pm 3.2$	> 14.79	$14.73 \pm 0.01$
	1550.7700	−1.0213	ESI	[−120, 350]	$739.1 \pm 10.9$	$14.73 \pm 0.01$	
N I							
	1134.4149	−1.5714	HIRES	[−80, 40]	$123.6 \pm 3.4$	$14.71 \pm 0.01$	$14.71 \pm 0.01$
	1200.2233	−1.0645	HIRES	[−50, 50]	$211.1 \pm 3.2$	> 14.63	
N II							
	1083.9900	−0.9867	HIRES	[−50, 50]	$213.6 \pm 4.0$	> 14.72	> 14.72
O I							
	1039.2304	−2.0364	HIRES	[−120, 45]	$399.8 \pm 9.0$	> 16.04	> 16.04
	1302.1685	−1.3110	HIRES	[−120, 120]	$778.8 \pm 2.3$	> 15.65	
Al II							
	1670.7874	0.2742	ESI	[−110, 360]	$830.8 \pm 3.0$	> 13.69	> 13.69
Al III							
	1854.7164	−0.2684	ESI	[−100, 320]	$195.8 \pm 4.9$	$13.14 \pm 0.01$	$13.13 \pm 0.01$
	1862.7895	−0.5719	ESI	[−100, 320]	$109.3 \pm 13.2$	$13.11 \pm 0.02$	
Si II							
	1190.4158	−0.6017	HIRES	[−120, 100]	$588.2 \pm 4.0$	> 14.75	> 15.02
	1526.7066	−0.8962	ESI	[−110, 110]	$700.9 \pm 10.3$	> 15.02	
Si IV							
	1393.7550	−0.2774	HIRES	[−130, 330]	$634.5 \pm 13.9$	> 14.11	$14.06 \pm 0.01$
	1402.7700	−0.5817	HIRES	[−130, 330]	$385.9 \pm 17.3$	$14.06 \pm 0.01$	
Ar I							
	1066.6600	−1.1709	HIRES	[−40, 40]	< 12.2	< 13.44	< 13.44
Cr II							
	2056.2539	−0.9788	ESI	[−50, 50]	$35.9 \pm 2.9$	< 12.98	< 12.61
	2066.1610	−1.2882	ESI	[−50, 50]	< 5.2	< 12.61	
Fe II							
	1608.4511	−1.2366	ESI	[−120, 120]	$266.2 \pm 2.5$	$14.48 \pm 0.01$	$14.48 \pm 0.01$
	1611.2005	−2.8665	ESI	[−120, 120]	< 5.6	< 14.43	
Ni II							

Table 10—Continued

Ion	$\lambda$ (Å)	$\log f$	Instr.	$v_{int}^a$ (km s $^{-1}$ )	$W_\lambda^b$ (mÅ)	$\log N$	$\log N_{adopt}$
Zn II	1370.1310	−1.2306	HIRES	[−20, 30]	$14.8 \pm 1.3$	$13.20 \pm 0.04$	$13.27 \pm 0.03$
	1751.9157	−1.5575	ESI	[−50, 60]	$21.5 \pm 2.1$	$13.47 \pm 0.04$	
	2026.1360	−0.3107	ESI	[−20, 50]	< 27.4	$12.18 \pm 0.04$	$12.18 \pm 0.04$
	2062.6640	−0.5918	ESI	[−50, 50]	$18.4 \pm 2.7$	< 12.29	

<sup>a</sup>Velocity interval over which the equivalent width and column density are measured.

<sup>b</sup>Rest equivalent width.

Table 11. IONIC COLUMN DENSITIES FOR J2340-00  $z = 2.05452$ 

Ion	$\lambda$ (Å)	$\log f$	Instr.	$v_{int}^a$ (km s $^{-1}$ )	$W_\lambda^b$ (mÅ)	$\log N$	$\log N_{adopt}$
C I							
	1560.3092	-0.8808	HIRES	[−50, 40]	$64.3 \pm 3.3$	$> 13.44$	$> 13.63$
	1656.9283	-0.8273	HIRES	[−40, 30]	$113.5 \pm 4.8$	$> 13.63$	
C II							
	1334.5323	-0.8935	HIRES	[−200, 120]	$913.8 \pm 12.7$	$> 15.20$	$> 15.20$
	1335.7077	-0.9397	HIRES	[−80, 100]	$105.4 \pm 9.0$	$13.84 \pm 0.04$	
C IV							
	1548.1950	-0.7194	HIRES	[−220, 130]	$326.9 \pm 7.9$	$14.00 \pm 0.01$	$14.02 \pm 0.01$
	1550.7700	-1.0213	HIRES	[−220, 130]	$205.6 \pm 8.1$	$14.06 \pm 0.02$	
O I							
	1302.1685	-1.3110	HIRES	[−200, 120]	$752.7 \pm 16.4$	$> 15.45$	$> 15.45$
Al II							
	1670.7874	0.2742	HIRES	[−120, 120]	$782.1 \pm 16.6$	$> 13.75$	$> 13.75$
Al III							
	1854.7164	-0.2684	HIRES	[−120, 100]	$217.9 \pm 6.2$	$13.19 \pm 0.01$	$13.17 \pm 0.01$
	1862.7895	-0.5719	HIRES	[−120, 100]	$94.5 \pm 7.2$	$13.10 \pm 0.03$	
Si II							
	1304.3702	-1.0269	HIRES	[−160, 100]	$621.4 \pm 12.9$	$> 15.08$	$15.17 \pm 0.04$
	1526.7066	-0.8962	HIRES	[−120, 120]	$748.2 \pm 8.0$	$> 15.00$	
	1808.0130	-2.6603	HIRES	[−100, 100]	$84.2 \pm 7.8$	$15.17 \pm 0.04$	
Si IV							
	1393.7550	-0.2774	HIRES	[−100, 120]	$224.3 \pm 15.9$	$13.43 \pm 0.02$	$13.44 \pm 0.02$
	1402.7700	-0.5817	HIRES	[−100, 120]	$114.5 \pm 8.7$	$13.45 \pm 0.03$	
Cr II							
	2056.2539	-0.9788	HIRES	[−60, 80]	$83.8 \pm 5.6$	$< 13.36$	$< 12.90$
	2062.2340	-1.1079	HIRES	[−100, 50]	$20.5 \pm 6.8$	$< 12.90$	
Fe II							
	1608.4511	-1.2366	HIRES	[−140, 100]	$571.4 \pm 7.7$	$> 14.97$	$> 14.97$
Ni II							
	1317.2170	-1.2434	HIRES	[−100, 100]	$47.2 \pm 13.6$	$13.79 \pm 0.12$	$13.78 \pm 0.03$
	1370.1310	-1.2306	HIRES	[−100, 100]	$41.2 \pm 9.6$	$13.70 \pm 0.09$	
	1454.8420	-1.4908	HIRES	[−100, 100]	$< 18.0$	$13.69 \pm 0.14$	
	1741.5531	-1.3696	HIRES	[−100, 120]	$70.8 \pm 6.6$	$13.82 \pm 0.04$	
	1751.9157	-1.5575	HIRES	[−100, 120]	$< 16.3$	$< 13.51$	
Zn II							
	2026.1360	-0.3107	HIRES	[−70, 100]	$102.3 \pm 6.6$	$< 12.80$	$12.63 \pm 0.08$

Table 11—Continued

Ion	$\lambda$ (Å)	$\log f$	Instr.	$v_{int}^a$ (km s <sup>-1</sup> )	$W_\lambda^b$ (mÅ)	$\log N$	$\log N_{adopt}$

<sup>a</sup>Velocity interval over which the equivalent width and column density are measured.

<sup>b</sup>Rest equivalent width.

Table 12. IONIC COLUMN DENSITIES FOR Q2342+34  $z = 2.90823$ 

Ion	$\lambda$ (Å)	$\log f$	Instr.	$v_{int}^a$ (km s $^{-1}$ )	$W_\lambda^b$ (mÅ)	$\log N$	$\log N_{adopt}$
C I	1560.3092	-0.8808	HIRES	[0, 120]	< 15.3	< 12.92	< 12.68
	1656.9283	-0.8273	HIRES	[0, 100]	< 11.3	< 12.68	
C II	1334.5323	-0.8935	HIRES	[-50, 240]	$862.8 \pm 10.9$	$> 15.15$	$> 15.15$
	1335.7077	-0.9397	HIRES	[0, 130]	$62.9 \pm 8.2$	$13.61 \pm 0.06$	
C IV	1548.1950	-0.7194	HIRES	[-90, 280]	$662.4 \pm 9.6$	$> 14.43$	$14.46 \pm 0.01$
	1550.7700	-1.0213	HIRES	[-90, 280]	$431.4 \pm 10.1$	$14.46 \pm 0.01$	
N I	1134.9803	-1.3954	ESI	[-60, 80]	$239.8 \pm 16.8$	$14.90 \pm 0.04$	$14.92 \pm 0.04$
O I	1302.1685	-1.3110	HIRES	[-50, 210]	$738.1 \pm 7.4$	$> 15.53$	$> 15.53$
Mg II	1240.3947	-3.4498	ESI	[-20, 60]	< 14.9	< 15.68	< 15.68
Al II	1670.7874	0.2742	ESI	[-100, 200]	$752.2 \pm 15.9$	$> 13.62$	$> 13.62$
Al III	1854.7164	-0.2684	ESI	[-60, 120]	$192.9 \pm 14.8$	$13.13 \pm 0.04$	$13.13 \pm 0.04$
Si II	1260.4221	0.0030	HIRES	[-40, 250]	$844.5 \pm 5.5$	$> 14.36$	$15.62 \pm 0.02$
	1304.3702	-1.0269	HIRES	[0, 210]	$569.9 \pm 6.8$	$> 15.09$	
	1526.7066	-0.8962	HIRES	[0, 200]	$757.4 \pm 19.1$	$> 14.94$	
	1808.0126	-2.6603	HIRES	[0, 150]	$210.1 \pm 9.1$	$15.62 \pm 0.02$	
Si IV	1393.7550	-0.2774	HIRES	[10, 280]	$507.3 \pm 12.6$	$> 14.01$	$14.04 \pm 0.01$
	1402.7700	-0.5817	HIRES	[0, 280]	$376.8 \pm 16.2$	$14.04 \pm 0.01$	
S II	1259.5190	-1.7894	HIRES	[0, 150]	$238.8 \pm 4.6$	$15.19 \pm 0.01$	$15.19 \pm 0.01$
Cr II	2056.2539	-0.9788	ESI	[-60, 100]	$84.1 \pm 15.2$	$13.36 \pm 0.08$	$13.36 \pm 0.08$
Fe II	1121.9748	-1.6946	ESI	[-30, 150]	$171.9 \pm 21.8$	$15.02 \pm 0.06$	$15.02 \pm 0.06$
	1608.4511	-1.2366	ESI	[-20, 200]	$474.6 \pm 11.2$	$> 14.88$	
	1611.2005	-2.8665	ESI	[-20, 150]	< 22.3	< 15.03	
	2249.8768	-2.7397	ESI	[-35, 100]	$119.2 \pm 22.4$	< 15.22	

Table 12—Continued

Ion	$\lambda$ (Å)	$\log f$	Instr.	$v_{int}^a$ (km s <sup>-1</sup> )	$W_\lambda^b$ (mÅ)	$\log N$	$\log N_{adopt}$
Ni II	2344.2140	−0.9431	ESI	[−30, 200]	$954.1 \pm 24.3$	$> 14.67$	
	1317.2170	−1.2434	HIRES	[0, 150]	$68.1 \pm 8.1$	$13.94 \pm 0.05$	$13.82 \pm 0.03$
	1709.6042	−1.4895	HIRES	[0, 120]	$43.8 \pm 7.2$	$13.76 \pm 0.07$	
	1741.5531	−1.3696	HIRES	[0, 120]	$56.4 \pm 8.1$	$13.74 \pm 0.06$	
Zn II	1751.9157	−1.5575	ESI	[−30, 120]	$56.5 \pm 11.1$	$13.90 \pm 0.09$	
	2026.1360	−0.3107	ESI	[−20, 140]	$< 35.9$	$< 12.47$	$< 12.47$

<sup>a</sup>Velocity interval over which the equivalent width and column density are measured.

<sup>b</sup>Rest equivalent width.

Table 13. DLA METAL SUMMARY

Quasar	RA (2000)	DEC (2000)	$z_{em}$	$z_{abs}$	$\log N_{\text{HI}}$	$f_{\alpha}^a$	[ $\alpha/\text{H}$ ]	$\sigma(\alpha)$	$f_{Zn}^b$	[Zn/H]	$\sigma(\text{Zn})$	$f_{Fe}^c$	[Fe/H]	$\sigma(\text{Fe})$	Ref
SDSS1435+0420	14:35:12.94	+04:20:36	1.950	1.6559	$21.25^{+0.15}_{-0.15}$	1	-0.89	0.07	3	-0.55		1	-1.05	0.07	29
Q1104-18	11:06:32.96	-18:21:09.82	2.310	1.6614	$20.80^{+0.10}_{-0.10}$	1	-1.04	0.01	1	-0.99	0.01	1	-1.48	0.02	7
Q1331+17	13:33:35.78	+16:49:04.03	2.080	1.7764	$21.14^{+0.08}_{-0.08}$	1	-1.42	0.00	1	-1.27	0.03	1	-2.02	0.00	6,13
SDSS1249-0233	12:49:24.86	-02:33:39	2.120	1.7806	$21.45^{+0.15}_{-0.15}$	1	-1.21	0.03	1	-1.01	0.04	1	-1.48	0.02	29
B2314-409	23:16:46.94	-40:41:21.3	2.448	1.8573	$20.90^{+0.10}_{-0.10}$	1	-1.05	0.11	1	-1.05	0.11	1	-1.32	0.11	22
Q0841+12	08:44:24.289	+12:45:48.74	2.500	1.8640	$21.00^{+0.10}_{-0.10}$	4	-1.51	0.03	0			0			26
Q2230+02	22:32:35.30	+02:47:55.12	2.150	1.8644	$20.85^{+0.08}_{-0.08}$	1	-0.75	0.01	1	-0.72	0.03	1	-1.16	0.02	6,13
Q1210+17	12:13:03.07	+17:14:23.01	2.540	1.8918	$20.60^{+0.10}_{-0.10}$	1	-0.87	0.02	1	-0.90	0.03	1	-1.14	0.06	13,30
B1055-301	10:58:00.41	-30:24:55.5	2.523	1.9035	$21.54^{+0.10}_{-0.10}$	0			1	-1.30	0.03	5	-1.80	0.02	27
CTQ247	04:07:18.0	-44:10:29.7	3.020	1.9130	$20.80^{+0.10}_{-0.10}$	0			1	-1.03	0.03	0			26
Q2206-19	22:08:52.05	-19:43:57.61	2.560	1.9200	$20.65^{+0.07}_{-0.07}$	1	-0.42	0.00	1	-0.41	0.01	1	-0.86	0.02	4,6,13
B1230-101	12:33:13.16	-10:25:18.4	2.394	1.9314	$20.48^{+0.10}_{-0.10}$	0			1	-0.22	0.05	5	-0.68	0.04	27
Q1157+014	11:59:44.81	+01:12:07.1	1.990	1.9440	$21.80^{+0.10}_{-0.10}$	2	-1.43		1	-1.36	0.06	1	-1.81	0.04	9
B0347-211	03:49:57.82	-21:02:47.7	2.944	1.9470	$20.30^{+0.10}_{-0.10}$	0			3	-0.59		0			27
Q0551-366	05:52:46.19	-36:37:28.5	2.318	1.9622	$20.50^{+0.08}_{-0.08}$	1	-0.44	0.06	1	-0.15	0.05	1	-0.95	0.05	17,18
SDSS0016-0012	00:16:02.40	-00:12:24.9	2.090	1.9700	$20.83^{+0.15}_{-0.15}$	1	-0.91	0.11	1	-0.44	0.08	1	-1.43	0.01	29,30
Q0013-004	00:16:02.40	-00:12:25.0	2.086	1.9730	$20.83^{+0.07}_{-0.07}$	1	-0.96	0.04	1	-0.76	0.08	1	-1.52	0.04	24
Q1215+33	12:17:32.54	+33:05:38.39	2.610	1.9991	$20.95^{+0.07}_{-0.07}$	1	-1.48	0.03	1	-1.29	0.05	1	-1.70	0.05	6,13
Q1409+095	14:12:17	+09:16:25	2.838	2.0190	$20.65^{+0.10}_{-0.10}$	0			1	-1.62	0.15	0			26
Q0010-002	00:13:06.15	+00:04:31.9	2.145	2.0250	$20.80^{+0.10}_{-0.10}$	0			1	-1.20	0.06	1	-1.33	0.04	24
Q0458-02	05:01:12.81	-01:59:14.25	2.290	2.0396	$21.65^{+0.09}_{-0.09}$	2	-1.17		1	-1.19	0.02	1	-1.76	0.05	6,13
J2340-00	23:40:23.7	-00:53:27.0	2.090	2.0545	$20.35^{+0.15}_{-0.15}$	1	-0.74	0.04	1	-0.39	0.08	4	-0.92	0.03	29,31
Q2231-002	22:34:08.80	+00:00:02.00	3.020	2.0661	$20.56^{+0.10}_{-0.10}$	1	-0.88	0.02	1	-0.88	0.03	1	-1.40	0.07	2,6,13,25
Q0450-13	04:53:13.75	-13:05:54.4	2.300	2.0666	$20.53^{+0.08}_{-0.08}$	1	-1.47	0.01	0			1	-1.88	0.03	13
FJ0812+32	08:12:40.8	+32:08:08	2.670	2.0668	$21.00^{+0.10}_{-0.10}$	1	-1.38	0.01	1	-1.46	0.02	1	-1.61	0.02	22,31
Q2206-19	22:08:52.05	-19:43:57.61	2.560	2.0762	$20.43^{+0.06}_{-0.06}$	1	-2.31	0.04	3	-1.86		1	-2.61	0.02	4,6,13
Q2359-02	00:01:50.00	-01:59:40.34	2.800	2.0951	$20.70^{+0.10}_{-0.10}$	1	-0.77	0.02	1	-0.77	0.03	1	-1.65	0.03	6,13
Q0135-273	01:37:54.49	-27:07:35.80	3.210	2.1070	$20.30^{+0.15}_{-0.15}$	4	-1.12	0.08	0			0			26
Q0149+33	01:52:34.472	+33:50:33.23	2.430	2.1408	$20.50^{+0.10}_{-0.10}$	1	-1.49	0.05	1	-1.69	0.12	1	-1.77	0.02	6,13
Q0528-2505	05:30:07.96	-25:03:29.90	2.780	2.1410	$20.95^{+0.05}_{-0.05}$	1	-1.25	0.04	0			1	-1.51	0.36	2
Q2359-02	00:01:50.00	-01:59:40.34	2.800	2.1539	$20.30^{+0.10}_{-0.10}$	1	-1.58	0.01	3	-1.06		1	-1.88	0.03	6,13
B2311-373	23:13:59.71	-37:04:45.4	2.476	2.1821	$20.48^{+0.10}_{-0.10}$	0			3	-1.33		0			27
B1223-113	12:30:55.62	-11:39:09.9	3.528	2.1929	$20.60^{+0.10}_{-0.10}$	0			1	-0.26	0.03	5	-1.02	0.03	27
SDSS2059-0529	20:59:22.42	-05:28:42	2.540	2.2100	$20.80^{+0.20}_{-0.20}$	1	-1.00	0.10	1	-0.53	0.11	1	-1.30	0.11	29
Q1451+123	14:54:18.61	+12:10:54.80	3.250	2.2550	$20.35^{+0.10}_{-0.10}$	0			1	-1.07	0.15	0			26

Table 13—Continued

Quasar	RA (2000)	DEC (2000)	$z_{em}$	$z_{abs}$	$\log N_{\text{HI}}$	$f_{\alpha}^a$	[ $\alpha/\text{H}$ ]	$\sigma(\alpha)$	$f_{Zn}^b$	[Zn/H]	$\sigma(\text{Zn})$	$f_{Fe}^c$	[Fe/H]	$\sigma(\text{Fe})$	Ref
SDSS1042+0117	10:42:52.32	+01:17:36	2.440	2.2668	$20.75^{+0.15}_{-0.15}$	1	-0.84	0.09	3	-0.68		1	-1.17	0.13	29
Q2348-14	23:51:29.91	-14:27:47.55	2.940	2.2794	$20.56^{+0.08}_{-0.08}$	1	-1.92	0.02	0			1	-2.24	0.02	6,13
Q0216+08	02:18:57.34	+08:17:27.75	3.000	2.2931	$20.45^{+0.16}_{-0.16}$	1	-0.56	0.04	0			1	-1.06	0.09	2
B0432-440	04:34:03.23	-43:55:47.8	2.649	2.3020	$20.78^{+0.10}_{-0.10}$	0			3	-1.25		5	-1.54	0.06	27
PH957	01:03:11.38	+13:16:16.7	2.690	2.3090	$21.37^{+0.08}_{-0.08}$	4	-1.46	0.01	1	-1.59	0.02	1	-1.90	0.04	1,6,13
HE2243-6031	22:46:11.00	-60:15:12.00	3.010	2.3300	$20.67^{+0.02}_{-0.02}$	1	-0.87	0.03	0			1	-1.25	0.03	18
Q1232+08	12:34:37.55	+07:58:40.5	2.570	2.3371	$20.90^{+0.10}_{-0.10}$	1	-1.28	0.09	0			1	-1.72	0.09	9
B0438-436	04:40:17.18	-43:33:08.6	2.863	2.3474	$20.78^{+0.10}_{-0.10}$	0			1	-0.73	0.03	5	-1.57	0.05	27
SDSS2222-0946	22:22:56.11	-09:46:36	2.927	2.3543	$20.50^{+0.15}_{-0.15}$	1	-0.61	0.05	3	-0.39		1	-1.05	0.02	29
Q0102-190	01:05:16.80	-18:46:42.10	3.037	2.3700	$20.85^{+0.10}_{-0.10}$	4	-1.81	0.05	0			1	-1.89	0.08	24
Q0841+12	08:44:24.289	+12:45:48.74	2.500	2.3745	$20.95^{+0.09}_{-0.09}$	1	-1.27	0.02	1	-1.50	0.05	4	-1.78	0.03	6,13
Q2138-444	21:41:59.79	-44:13:25.90	3.170	2.3830	$20.60^{+0.05}_{-0.05}$	0			1	-1.15	0.10	0			26
Q0112-306	01:14:51.40	-30:14:09.00	2.985	2.4180	$20.50^{+0.08}_{-0.08}$	1	-2.45	0.05	0			1	-2.65	0.05	24
Q0112+029	01:14:34.90	+03:09:51	2.810	2.4230	$20.78^{+0.08}_{-0.08}$	4	-1.29	0.08	0			1	-1.46	0.05	24
Q2348-01	23:50:57.84	-00:52:10.07	3.014	2.4263	$20.50^{+0.10}_{-0.10}$	1	-0.69	0.02	0			1	-1.38	0.01	13
Q2343+125	23:46:28.22	+12:48:59.9	2.763	2.4313	$20.34^{+0.10}_{-0.10}$	1	-0.54	0.01	0			1	-1.20	0.00	5
Q1409+095	14:12:17	+09:16:25	2.838	2.4562	$20.54^{+0.10}_{-0.10}$	1	-2.02	0.02	0			1	-2.30	0.02	24
Q0201+36	02:04:55.60	+36:49:18.00	2.490	2.4628	$20.38^{+0.05}_{-0.05}$	1	-0.41	0.01	1	-0.29	0.05	1	-0.87	0.00	3,13
Q0836+11	08:39:33.015	+11:12:03.82	2.700	2.4653	$20.58^{+0.10}_{-0.10}$	1	-1.15	0.05	3	-1.12		1	-1.40	0.01	13
Q1223+17	12:26:07.22	+17:36:48.98	2.920	2.4661	$21.50^{+0.10}_{-0.10}$	1	-1.59	0.01	1	-1.62	0.03	1	-1.84	0.02	8,13
Q1451+123	14:54:18.61	+12:10:54.80	3.250	2.4690	$20.39^{+0.10}_{-0.10}$	1	-2.13	0.10	0			1	-2.46	0.05	24
Q0841+12	08:44:24.289	+12:45:48.74	2.500	2.4762	$20.78^{+0.10}_{-0.10}$	4	-1.39	0.03	3	-1.33		1	-1.75	0.05	6,13
B1354-107	13:56:33.62	-11:00:40.7	3.006	2.5009	$20.40^{+0.10}_{-0.10}$	0			3	-1.37		5	-1.40	0.04	27
SDSS1610+4724	16:10:09.42	+47:24:44	3.216	2.5082	$21.15^{+0.15}_{-0.15}$	2	-0.56		1	-0.29	0.02	1	-1.08	0.04	29
Q2344+12	23:46:45.79	+12:45:29.98	2.790	2.5379	$20.36^{+0.10}_{-0.10}$	1	-1.74	0.01	0			1	-1.82	0.03	2,13
CTQ247	04:07:18.0	-44:10:29.7	3.020	2.5505	$21.13^{+0.10}_{-0.10}$	1	-1.37	0.04	1	-1.36	0.05	1	-1.68	0.06	19
B0405-331	04:07:33.91	-33:03:46.4	2.570	2.5693	$20.60^{+0.10}_{-0.10}$	0			3	-0.53		0			27
Q1502+4837	15:02:27.34	+48:37:09.1	3.200	2.5696	$20.30^{+0.15}_{-0.15}$	1	-1.63	0.09	0			1	-1.65	0.12	22
Q1209+0919	12:11:34.93	+09:02:22.8	3.297	2.5841	$21.40^{+0.10}_{-0.10}$	1	-1.05	0.01	1	-1.09	0.05	1	-1.65	0.03	31
CTQ247	04:07:18.0	-44:10:29.7	3.020	2.5950	$21.09^{+0.10}_{-0.10}$	1	-1.06	0.03	1	-1.08	0.02	1	-1.44	0.02	22
Q2348-01	23:50:57.84	-00:52:10.07	3.014	2.6147	$21.30^{+0.10}_{-0.10}$	1	-1.98	0.07	3	-2.07		1	-2.23	0.09	13
Q0913+072	09:16:14.000	+07:02:24.6	2.785	2.6180	$20.35^{+0.10}_{-0.10}$	1	-2.60	0.05	0			0			26
CTQ247	04:07:18.0	-44:10:29.7	3.020	2.6215	$20.47^{+0.10}_{-0.10}$	1	-2.04	0.06	0			1	-2.37	0.02	22
Q1759+75	17:57:46.39	+75:39:16.01	3.050	2.6253	$20.76^{+0.01}_{-0.01}$	1	-0.79	0.01	2	-1.68		1	-1.18	0.00	6,13
FJ0812+32	08:12:40.8	+32:08:08	2.701	2.6263	$21.35^{+0.10}_{-0.10}$	1	-0.93	0.05	1	-0.87	0.02	1	-1.76	0.01	22,31

Table 13—Continued

Quasar	RA (2000)	DEC (2000)	$z_{em}$	$z_{abs}$	$\log N_{\text{HI}}$	$f_{\alpha}^a$	[ $\alpha/\text{H}$ ]	$\sigma(\alpha)$	$f_{Zn}^b$	[ $\text{Zn}/\text{H}$ ]	$\sigma(\text{Zn})$	$f_{Fe}^c$	[ $\text{Fe}/\text{H}$ ]	$\sigma(\text{Fe})$	Ref
Q0058-292	00:00:00.00	00:00:00.00	3.090	2.6710	$21.10^{+0.10}_{-0.10}$	1	-1.44	0.08	0			1	-1.86	0.06	24
B0933-333	09:35:09.23	-33:32:37.7	2.906	2.6823	$20.47^{+0.10}_{-0.10}$	0			3	-1.15		0			27
Q0112-306	01:14:51.40	-30:14:09.00	2.985	2.7020	$20.30^{+0.10}_{-0.10}$	1	-0.50	0.05	0			0			26
J1558-0031	15:58:10.16	-00:31:20.0	2.830	2.7026	$20.67^{+0.05}_{-0.05}$	1	-1.99	0.01	0			1	-2.06	0.03	28
SDSS0225+0054	02:25:54.85	+00:54:51	2.970	2.7144	$21.00^{+0.15}_{-0.15}$	1	-0.94	0.07	1	-0.78	0.11	1	-1.20	0.08	29
B0913+003	09:15:51.69	+00:07:13.3	3.074	2.7434	$20.74^{+0.10}_{-0.10}$	0			3	-0.59		5	-1.15	0.06	27
SDSS0844+5153	08:44:07.29	+51:53:11	3.200	2.7749	$21.45^{+0.15}_{-0.15}$	1	-1.04	0.02	0			1	-1.66	0.05	29
CTQ460	10:39:09.4	-23:13:26	3.130	2.7775	$21.00^{+0.10}_{-0.10}$	4	-1.37	0.02	3	-1.25		1	-1.82	0.01	22
PKS1354-17	13:57:05.87	-17:44:05.8	3.150	2.7799	$20.30^{+0.15}_{-0.15}$	1	-1.86	0.05	0			1	-2.33	0.08	22
PSS1253-0228	12:53:36.3	-02:28:08	4.010	2.7828	$21.85^{+0.20}_{-0.20}$	2	-1.81		1	-1.67	0.07	1	-2.01	0.04	22
HS1132+2243	11:35:08.03	+22:27:06.8	2.885	2.7835	$21.00^{+0.07}_{-0.07}$	1	-2.08	0.14	3	-1.62		1	-2.47	0.01	22
Q1337+11	13:40:02.44	+11:06:29.6	2.917	2.7959	$20.95^{+0.10}_{-0.10}$	1	-1.72	0.07	3	-1.37		1	-2.38	0.02	22,31
Q1008+36	10:08:41.31	+36:23:19.9	3.119	2.7989	$20.70^{+0.05}_{-0.05}$	1	-1.80	0.01	0			3	-1.09		13
Q0135-273	01:37:54.49	-27:07:35.80	3.210	2.8000	$21.00^{+0.10}_{-0.10}$	4	-1.57	0.08	0			1	-1.75	0.14	24
Q1425+6039	14:26:56.44	60:25:42.74	3.170	2.8268	$20.30^{+0.04}_{-0.04}$	2	-0.84		1	-0.79	0.04	1	-1.32	0.00	2,13,31
Q2138-444	21:41:59.79	-44:13:25.90	3.170	2.8520	$20.80^{+0.08}_{-0.08}$	0			1	-1.52	0.10	1	-1.72	0.05	24
Q2342+34	23:44:51.10	+34:33:46.8	2.917	2.9082	$21.10^{+0.10}_{-0.10}$	1	-1.04	0.02	3	-1.30		1	-1.58	0.06	22,31
Q1021+30	10:21:56.84	+30:01:31.3	3.120	2.9489	$20.70^{+0.10}_{-0.10}$	1	-1.94	0.02	3	-1.14		1	-2.16	0.01	13,22
B1354-107	13:56:33.62	-11:00:40.7	3.006	2.9668	$20.78^{+0.10}_{-0.10}$	0			3	-1.52		0			27
BRJ0426-2202	04:26:10.3	-22:02:17	4.320	2.9831	$21.50^{+0.15}_{-0.15}$	3	-1.97		3	-1.95		1	-2.75	0.06	22
HS0741+4741	07:45:21.75	+47:34:35.56	3.220	3.0174	$20.48^{+0.10}_{-0.10}$	1	-1.68	0.00	0			1	-1.93	0.00	13
Q0347-38	03:49:43.54	-38:10:04.91	3.230	3.0247	$20.63^{+0.00}_{-0.00}$	1	-1.16	0.03	0			1	-1.62	0.01	6,13,20
FJ2334-09	23:34:46.44	-09:08:11.8	3.330	3.0572	$20.45^{+0.10}_{-0.10}$	1	-1.08	0.07	3	-0.90		1	-1.62	0.01	22
Q0336-01	03:39:00.99	-01:33:18.07	3.200	3.0621	$21.20^{+0.10}_{-0.10}$	4	-1.54	0.01	0			1	-1.81	0.02	13
SDSS2100-0641	21:00:25.03	-06:41:46	3.140	3.0924	$21.05^{+0.15}_{-0.15}$	1	-0.72	0.01	3	-0.58		1	-1.19	0.03	29
BRI1013+0035	10:15:49.0	+00:20:20	4.405	3.1040	$21.10^{+0.10}_{-0.10}$	1	-0.88	0.02	1	-0.49	0.05	1	-1.42	0.05	31
PSS0808+52	08:08:49.53	+52:15:15.98	4.450	3.1132	$20.65^{+0.07}_{-0.07}$	1	-1.54	0.11	3	-1.14		1	-1.98	0.04	14,22
Q2223+20	22:25:37.01	+20:40:17.8	3.561	3.1192	$20.30^{+0.10}_{-0.10}$	1	-2.23	0.04	0			1	-2.37	0.04	22
B0347-211	03:37:55.40	-12:04:05.0	3.442	3.1799	$20.79^{+0.10}_{-0.10}$	0			3	-1.21		0			27
PSS1535+2943	15:35:53.9	+29:43:13.	3.990	3.2020	$20.65^{+0.15}_{-0.15}$	2	-1.47		3	-0.74		25	-1.41	0.15	23
PSS2315+0921	23:15:59.2	+09:21:44.	4.520	3.2191	$21.35^{+0.15}_{-0.15}$	0			3	-2.02		11	-2.02		22
PSS2344+0342	23:44:00	+03:42:00	4.240	3.2194	$21.35^{+0.07}_{-0.07}$	2	-1.99		3	-1.63		1	-1.56	0.08	22
PSS1506+5220	15:06:54.6	+52:20:05	4.180	3.2244	$20.67^{+0.07}_{-0.07}$	1	-2.33	0.02	3	-1.18		1	-2.45	0.04	22
Q0930+28	09:33:37.82	+28:45:35.26	3.420	3.2353	$20.30^{+0.10}_{-0.10}$	1	-1.97	0.02	0			1	-2.08	0.02	16
J0900+42	09:00:33.5	+42:15:46	3.290	3.2458	$20.30^{+0.10}_{-0.10}$	4	-0.85	0.00	0			1	-1.26	0.00	13,31

Table 13—Continued

Quasar	RA (2000)	DEC (2000)	$z_{em}$	$z_{abs}$	$\log N_{\text{HI}}$	$f_{\alpha}^a$	$[\alpha/\text{H}]$	$\sigma(\alpha)$	$f_{Zn}^b$	$[\text{Zn}/\text{H}]$	$\sigma(\text{Zn})$	$f_{Fe}^c$	$[\text{Fe}/\text{H}]$	$\sigma(\text{Fe})$	Ref
J0255+00	02:55:18.62	+00:48:47.94	3.970	3.2529	$20.70^{+0.10}_{-0.10}$	1	-0.93	0.04	0			1	-1.44	0.01	13
CTQ298	11:13:50.6	-15:33:34.0	3.370	3.2660	$21.30^{+0.05}_{-0.05}$	0			1	-1.65	0.11	0			26
PSS1432+39	14:32:24.93	+39:40:23.87	4.280	3.2725	$21.25^{+0.10}_{-0.10}$	1	-1.08	0.05	3	-1.21		4	-1.85	0.10	14,22
PSS0957+33	09:57:44.47	+33:08:23.46	4.250	3.2796	$20.45^{+0.08}_{-0.08}$	1	-1.13	0.05	3	-0.97		1	-1.58	0.02	14,13
PSS2155+1358	21:55:02.1	+13:58:26	4.260	3.3163	$20.55^{+0.15}_{-0.15}$	1	-1.23	0.07	3	-1.11		25	-1.59	0.15	22
Q1055+46	10:57:56.20	+45:55:44.31	4.130	3.3172	$20.34^{+0.10}_{-0.10}$	1	-1.65	0.11	0			1	-1.87	0.01	5
PSS1715+3809	17:15:39.6	+38:09:10	4.520	3.3407	$21.05^{+0.15}_{-0.10}$	3	-2.08		3	-1.55		1	-2.79	0.04	23
BR1117-1329	11:17:00	-13:29:00	3.960	3.3504	$20.84^{+0.10}_{-0.10}$	1	-1.27	0.08	1	-1.25	0.04	1	-1.51	0.03	24
Q0201+11	02:03:46.53	11:34:40.4	3.610	3.3869	$21.26^{+0.10}_{-0.10}$	4	-1.25	0.11	0			1	-1.41	0.05	15
Q0000-2619	00:03:22.909	-26:03:16.83	4.110	3.3901	$21.41^{+0.08}_{-0.08}$	1	-1.91	0.02	0			1	-2.16	0.03	2,6,10,12
PSS1802+5616	18:02:48.9	+56:16:51.	4.180	3.3913	$20.30^{+0.10}_{-0.10}$	13	-1.40	0.15	3	-0.51		1	-1.53	0.04	23
PC0953+47	09:56:25.17	+47:34:43.6	4.460	3.4036	$21.15^{+0.15}_{-0.15}$	13	-1.80	0.29	0			2	-2.18		22
FJ0747+2739	07:47:11.19	+27:39:03.6	4.110	3.4233	$20.85^{+0.05}_{-0.05}$	13	-1.66	0.21	0			11	-1.76		22
PSS2315+0921	23:15:59.2	+09:21:44.	4.520	3.4252	$21.10^{+0.20}_{-0.20}$	1	-1.51	0.05	0			11	-1.76		22
BR0019-15	00:22:08.01	-15:05:38.78	4.530	3.4389	$20.92^{+0.10}_{-0.10}$	1	-1.06	0.05	0			4	-1.58	0.04	6,13
B1418-064	14:21:07.76	-06:43:56.3	3.689	3.4483	$20.40^{+0.10}_{-0.10}$	0			3	-1.09		0			27
PSS0007+2417	00:07:38.7	+24:17:25.	4.050	3.4960	$21.10^{+0.10}_{-0.10}$	1	-1.57	0.04	3	-1.32		4	-1.78	0.04	23
PSS1802+5616	18:02:48.9	+56:16:51.	4.180	3.5539	$20.50^{+0.10}_{-0.10}$	2	-1.82		3	-0.56		1	-1.91	0.06	23
BRI1108-07	11:11:13.64	-08:04:02.47	3.920	3.6076	$20.50^{+0.10}_{-0.10}$	1	-1.80	0.00	0			1	-2.12	0.01	8,13
PSS0209+0517	02:09:44.52	+05:17:17.3	4.170	3.6667	$20.45^{+0.10}_{-0.10}$	13	-1.68	0.20	0			1	-2.31	0.06	22
PSS2323+2758	23:23:41.0	+27:58:01	4.180	3.6845	$20.95^{+0.10}_{-0.10}$	1	-2.59	0.03	0			1	-3.05	0.12	22
PSS0133+0400	01:33:40.4	+04:00:59	4.130	3.6926	$20.70^{+0.10}_{-0.15}$	13	-1.85	0.21	0			1	-2.63	0.06	22
PSS1723+2243	17:3:23.2	+22:43:58	4.520	3.6947	$20.50^{+0.15}_{-0.15}$	2	-1.20		1	-0.62	0.13	13	-1.16		22
PSS1248+31	12:48:20.26	+31:10:44.06	4.350	3.6970	$20.63^{+0.07}_{-0.07}$	1	-1.72	0.01	3	-0.63		1	-2.20	0.05	14,22
PSS0007+2417	00:07:38.7	+24:17:25.	4.050	3.7045	$20.55^{+0.15}_{-0.15}$	2	-1.74		0			11	-1.62		23
SDSS0127-00	01:27:00.69	-00:45:59	4.060	3.7274	$21.15^{+0.10}_{-0.10}$	13	-2.11	0.29	0			0			22
BRI1346-03	13:49:16.82	-03:37:15.06	3.990	3.7358	$20.72^{+0.10}_{-0.10}$	1	-2.33	0.01	0			6	-2.63	0.02	6,13
PSS0134+3317	01:34:21.63	+33:07:56.5	4.520	3.7609	$20.85^{+0.05}_{-0.05}$	2	-2.51		0			6	-2.71	0.03	22
PSS1535+2943	15:35:53.9	+29:43:13.	3.990	3.7612	$20.40^{+0.15}_{-0.15}$	1	-2.02	0.05	3	0.09		6	-2.30	0.05	23
PSS1802+5616	18:02:48.9	+56:16:51.	4.180	3.7617	$20.55^{+0.15}_{-0.15}$	13	-1.52	0.21	0			0			23
PSS0133+0400	01:33:40.4	+04:00:59	4.130	3.7736	$20.55^{+0.10}_{-0.15}$	1	-0.65	0.04	3	-0.12		4	-0.84	0.03	22
PSS1802+5616	18:02:48.9	+56:16:51.	4.180	3.8109	$20.35^{+0.20}_{-0.20}$	1	-2.03	0.10	0			1	-2.17	0.11	23
PSS0007+2417	00:07:38.7	+24:17:25.	4.050	3.8382	$20.85^{+0.15}_{-0.15}$	13	-2.17	0.24	0			1	-2.44	0.03	23
BR0951-04	09:53:55.69	-05:04:18.5	4.370	3.8567	$20.60^{+0.10}_{-0.10}$	2	-1.53		0			1	-2.00	0.06	6,13
PSS0209+0517	02:09:44.52	+05:17:17.3	4.170	3.8643	$20.55^{+0.10}_{-0.10}$	1	-2.66	0.04	0			6	-2.87	0.05	22

Table 13—Continued

Quasar	RA (2000)	DEC (2000)	$z_{em}$	$z_{abs}$	$\log N_{\text{HI}}$	$f_{\alpha}^a$	$[\alpha/\text{H}]$	$\sigma(\alpha)$	$f_{Zn}^b$	$[\text{Zn}/\text{H}]$	$\sigma(\text{Zn})$	$f_{Fe}^c$	$[\text{Fe}/\text{H}]$	$\sigma(\text{Fe})$	Ref
PC0953+47	09:56:25.17	+47:34:43.6	4.460	3.8910	$21.20^{+0.10}_{-0.10}$	13	-1.46	0.15	0			4	-1.70	0.06	22
FJ0747+2739	07:47:11.19	+27:39:03.6	4.110	3.9000	$20.50^{+0.10}_{-0.10}$	1	-2.01	0.01	3	-0.73		6	-2.45	0.03	22
J0255+00	02:55:18.62	+00:48:47.94	3.970	3.9146	$21.30^{+0.05}_{-0.05}$	4	-1.78	0.01	0			1	-2.05	0.09	13
BRI0952-01	09:55:00.10	-01:30:06.94	4.430	4.0244	$20.55^{+0.10}_{-0.10}$	0			0			1	-1.86	0.08	8,13
BR2237-0607	22:39:53.39	-05:52:20.78	4.560	4.0803	$20.52^{+0.11}_{-0.11}$	1	-1.87	0.02	0			1	-2.14	0.12	2
PSS0957+33	09:57:44.47	+33:08:23.46	4.250	4.1798	$20.70^{+0.10}_{-0.10}$	1	-1.70	0.01	0			1	-2.07	0.05	14,13
BR0951-04	09:53:55.69	-05:04:18.5	4.370	4.2029	$20.40^{+0.10}_{-0.10}$	1	-2.62	0.03	0			3	-2.57	6,13	
PSS1443+27	14:43:31.22	+27:24:37.23	4.410	4.2241	$20.80^{+0.10}_{-0.10}$	2	-0.93		0			1	-1.10	0.06	8,13
PC0953+47	09:56:25.2	+47:34:44	4.460	4.2442	$20.90^{+0.15}_{-0.15}$	1	-2.19	0.03	0			1	-2.52	0.08	22
PSS2241+1352	22:41:47.9	+13:52:03	4.440	4.2824	$21.15^{+0.10}_{-0.10}$	4	-1.76	0.03	0			11	-1.87	22	
BR1202-07	12:05:23.63	-07:42:29.91	4.690	4.3829	$20.60^{+0.14}_{-0.14}$	1	-1.81	0.02	0			1	-2.19	0.12	2
J0307-4945	03:07:22.85	-49:45:47.6	4.780	4.4679	$20.67^{+0.09}_{-0.09}$	1	-1.55	0.08	0			1	-1.96	0.21	11
SDSS1737+5828	17:12:27.74	+57:55:06	4.850	4.7430	$20.65^{+0.15}_{-0.15}$	0			0			1	-2.82	0.15	21

<sup>a</sup>0=No measurement; 1=Si measurement; 2=Si lower limit; 3=Si upper limit; 4=[S/H] ; 5=[O/H] ; 13=S+Si limits

| 39

<sup>b</sup>0=No measurement; 1=Zn measurement; 2=Zn lower limit; 3=Zn upper limit

<sup>c</sup>0=No measurement; 1=Fe measurement; 2=Fe lower limit; 3=Fe upper limit; 4=[Ni/H]-0.1dex; 5=[Cr/H] - 0.2dex; 6=[Al/H]; 11-16=Fe, Ni, Cr, Al limits; 25=Mean of Fe limits.

Note. — Note that none of the limits reported take into account the uncertainty in the  $N_{\text{HI}}$  value.

References. — 1: Wolfe *et al.* (1994); 2: Lu *et al.* (1996); 3: Prochaska & Wolfe (1996); 4: Prochaska & Wolfe (1997); 5: Lu, Sargent & Barlow (1999); 6: Prochaska & Wolfe (1999); 7: Lopez *et al.* (1999); 8: Prochaska & Wolfe (2000); 9: Petitjean, Srianand & Ledoux (2000); 10: Molaro *et al.* (2000); 11: Dessauges-Zavadsky *et al.* (2001); 12: Molaro *et al.* (2001); 13: Prochaska *et al.* (2001); 14: Prochaska, Gawiser & Wolfe (2001); 15: Ellison *et al.* (2001); 16: Prochaska *et al.* (2002); 17: Ledoux, Srianand & Petitjean (2002); 18: Lopez *et al.* (2002); 19: Levshakov *et al.* (2002); 20: Lopez & Ellison (2003); 21: Songaila & Cowie (2002); 22: Prochaska *et al.* (2003); 23: Prochaska, Castro & Djorgovski (2003); 24: Ledoux, Petitjean & Srianand (2003); 25: Dessauges-Zavadsky *et al.* (2004); 26: Ledoux *et al.* (2006); 27: Akerman *et al.* (2005); 28: O'Meara *et al.* (2006); 29: Herbert-Fort *et al.* (2006); 30: Dessauges-Zavadsky *et al.* (2006); 31: This paper

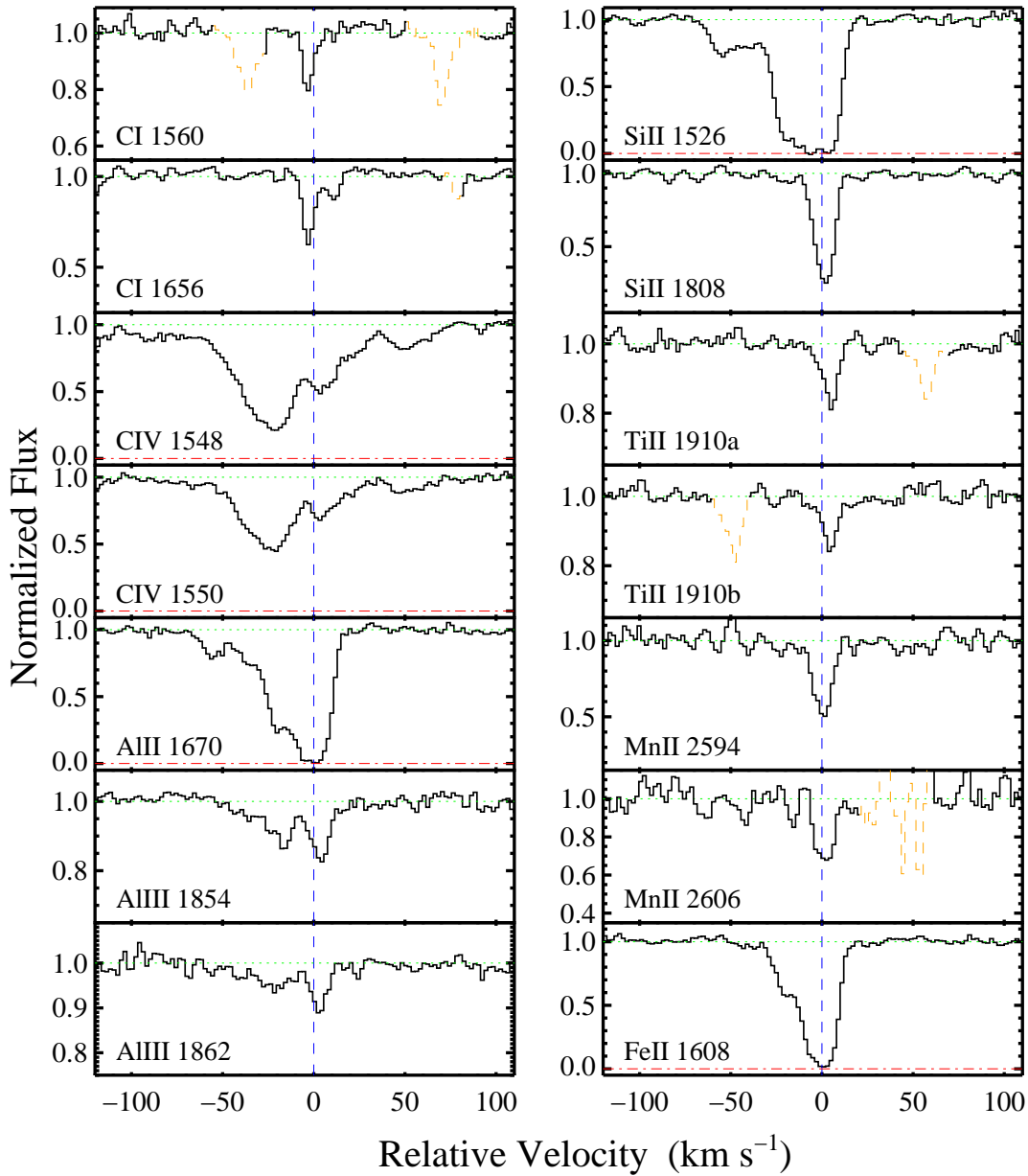
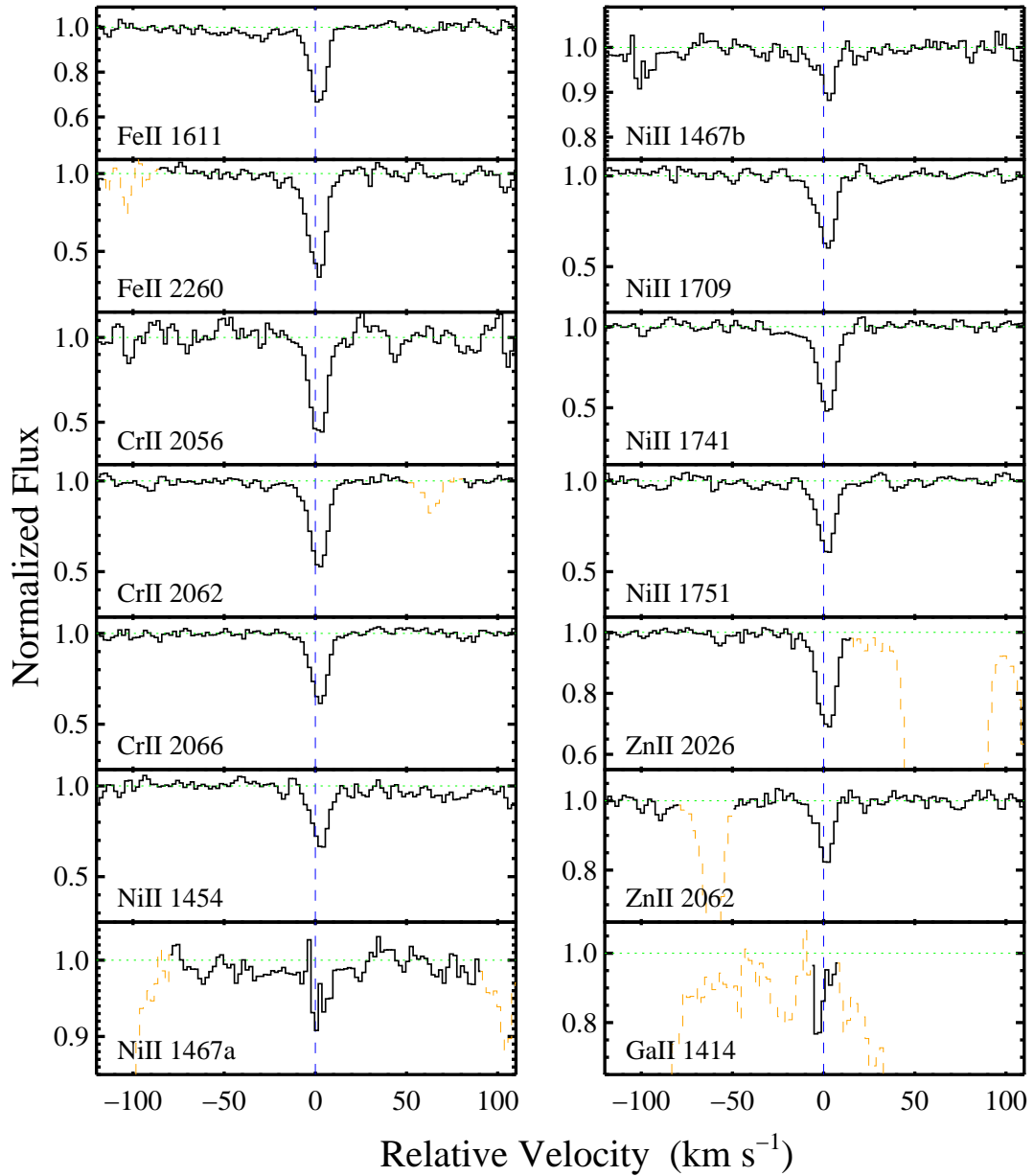


Fig. 1.— HIRES velocity profiles of the transitions identified with the damped Ly $\alpha$  systems at  $z = 2.0668$  toward FJ0812+32.



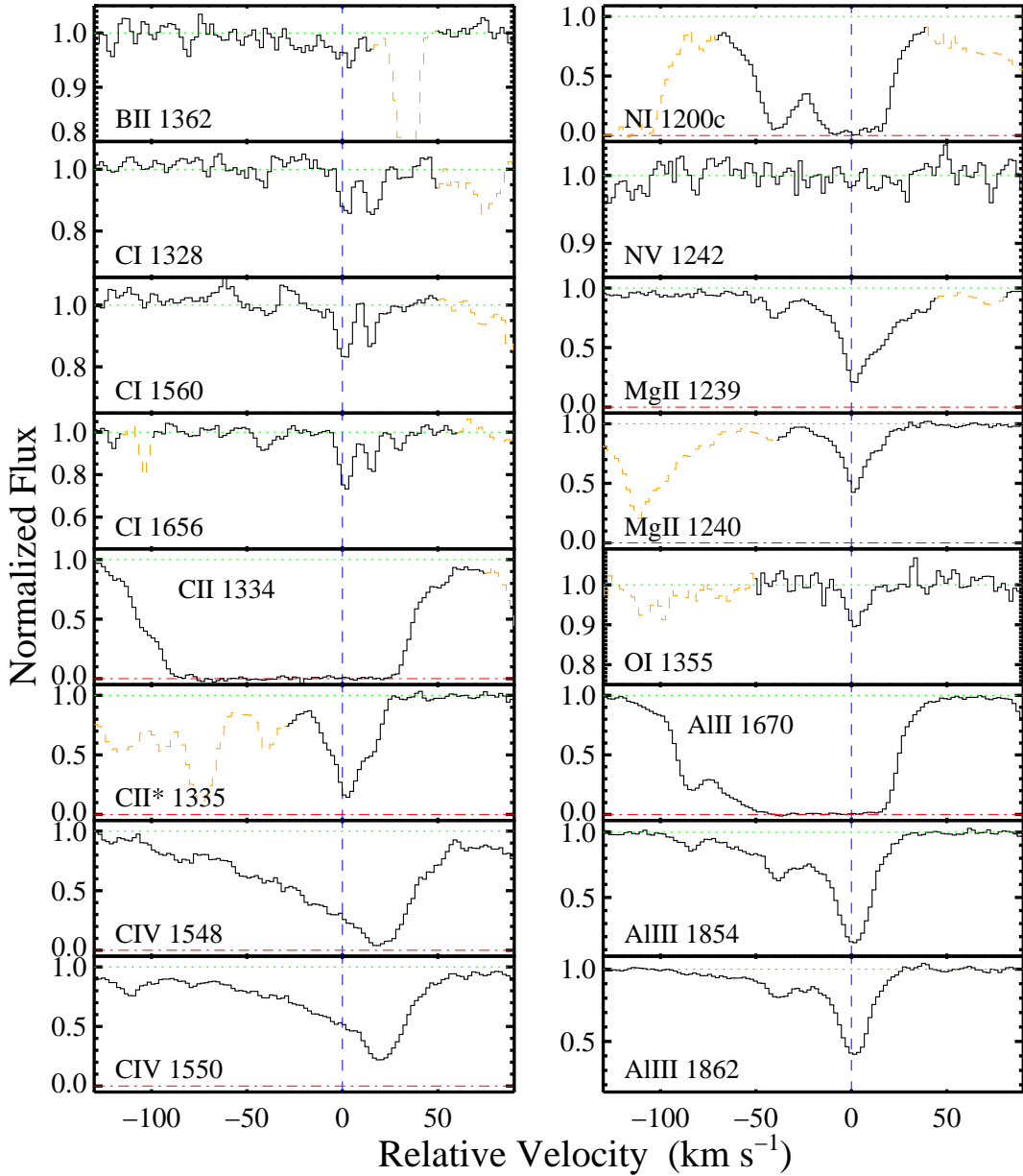
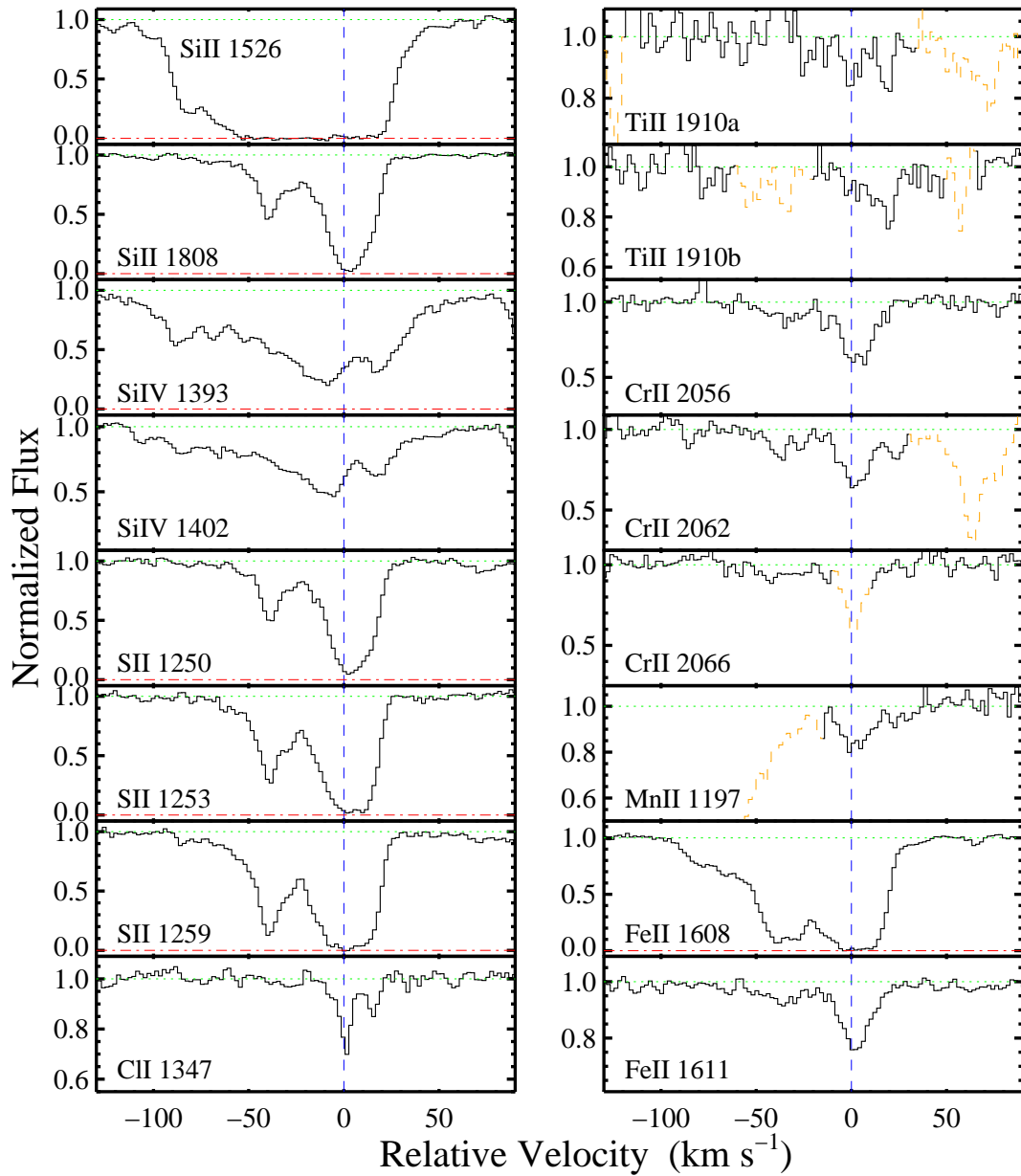
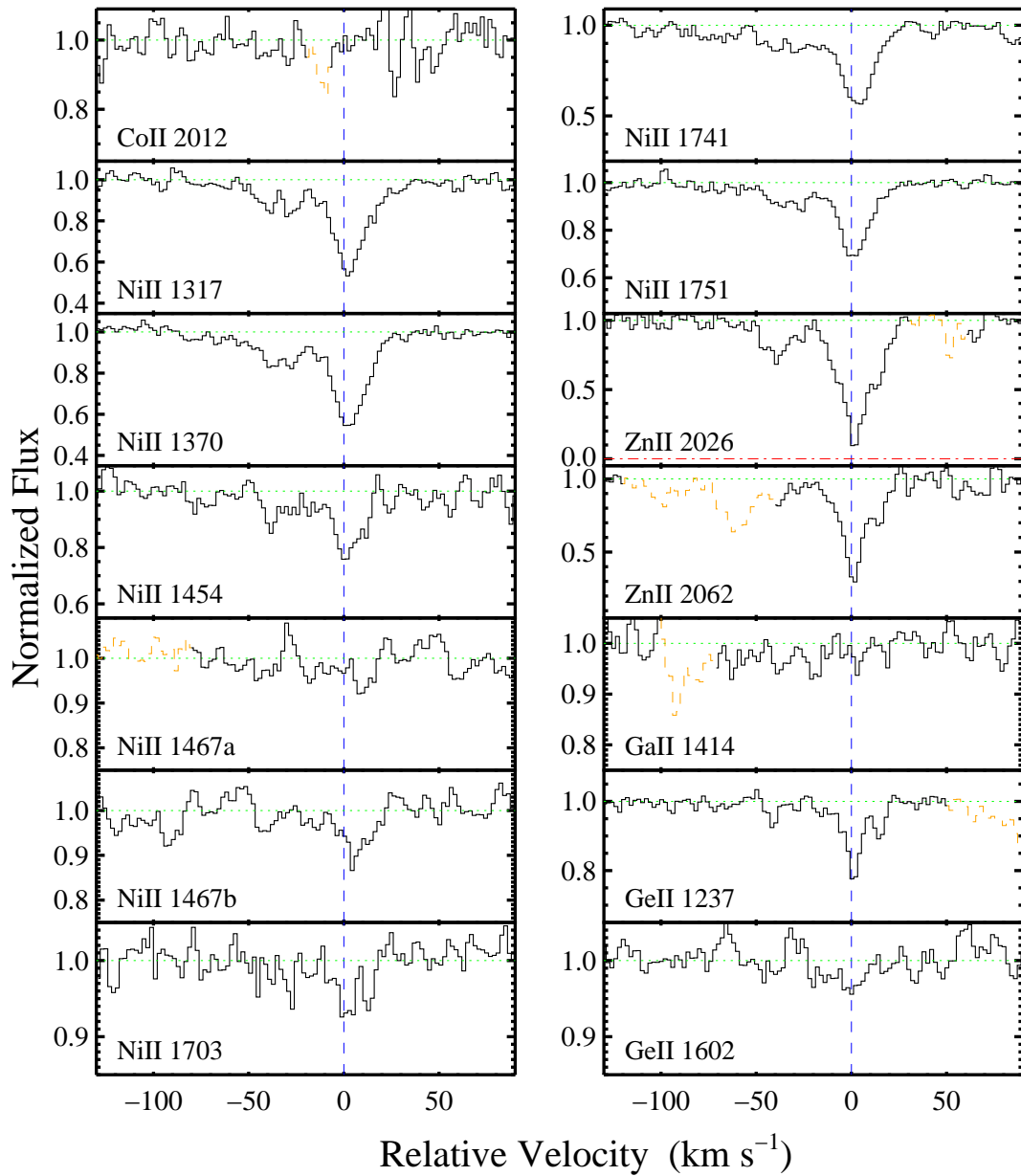


Fig. 2.— HIRES velocity profiles of the transitions identified with the damped Ly $\alpha$  systems at  $z = 2.6263$  toward FJ0812+32.





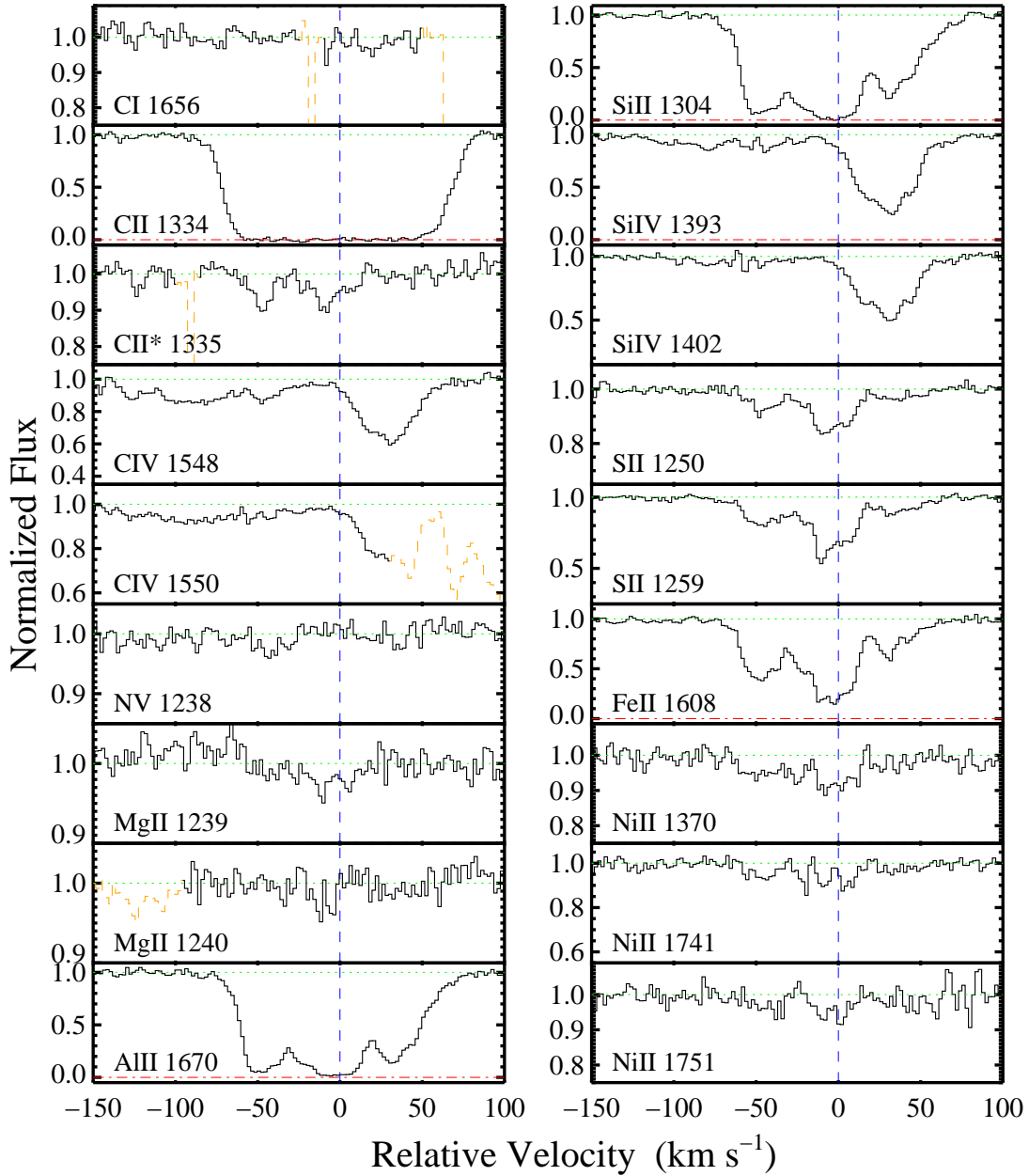


Fig. 3.— HIRES velocity profiles of the transitions identified with the damped Ly $\alpha$  systems at  $z = 3.2458$  toward J0900+42.

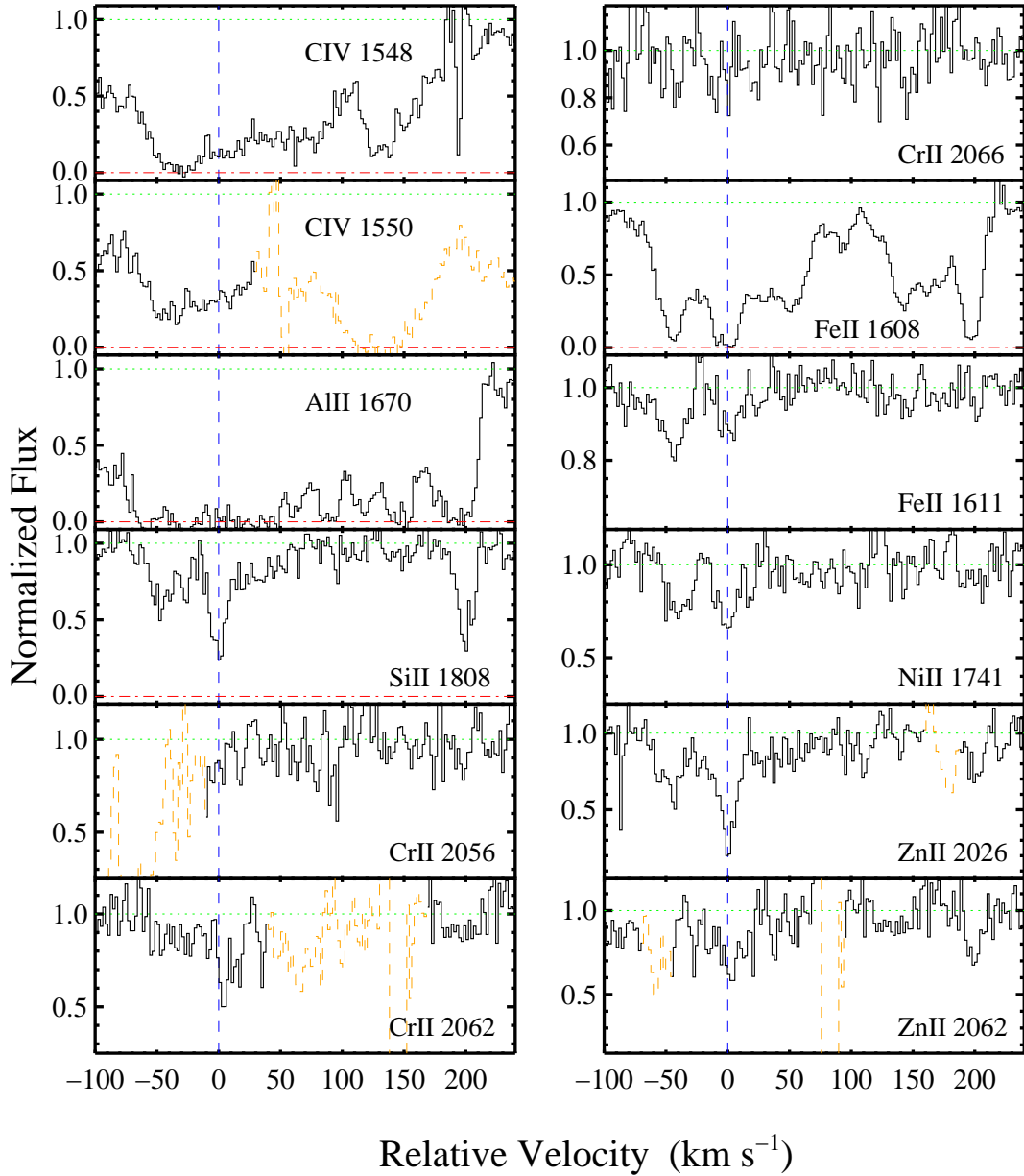


Fig. 4.— HIRES velocity profiles of the transitions identified with the damped Ly $\alpha$  systems at  $z = 3.1040$  toward B1013+0035.

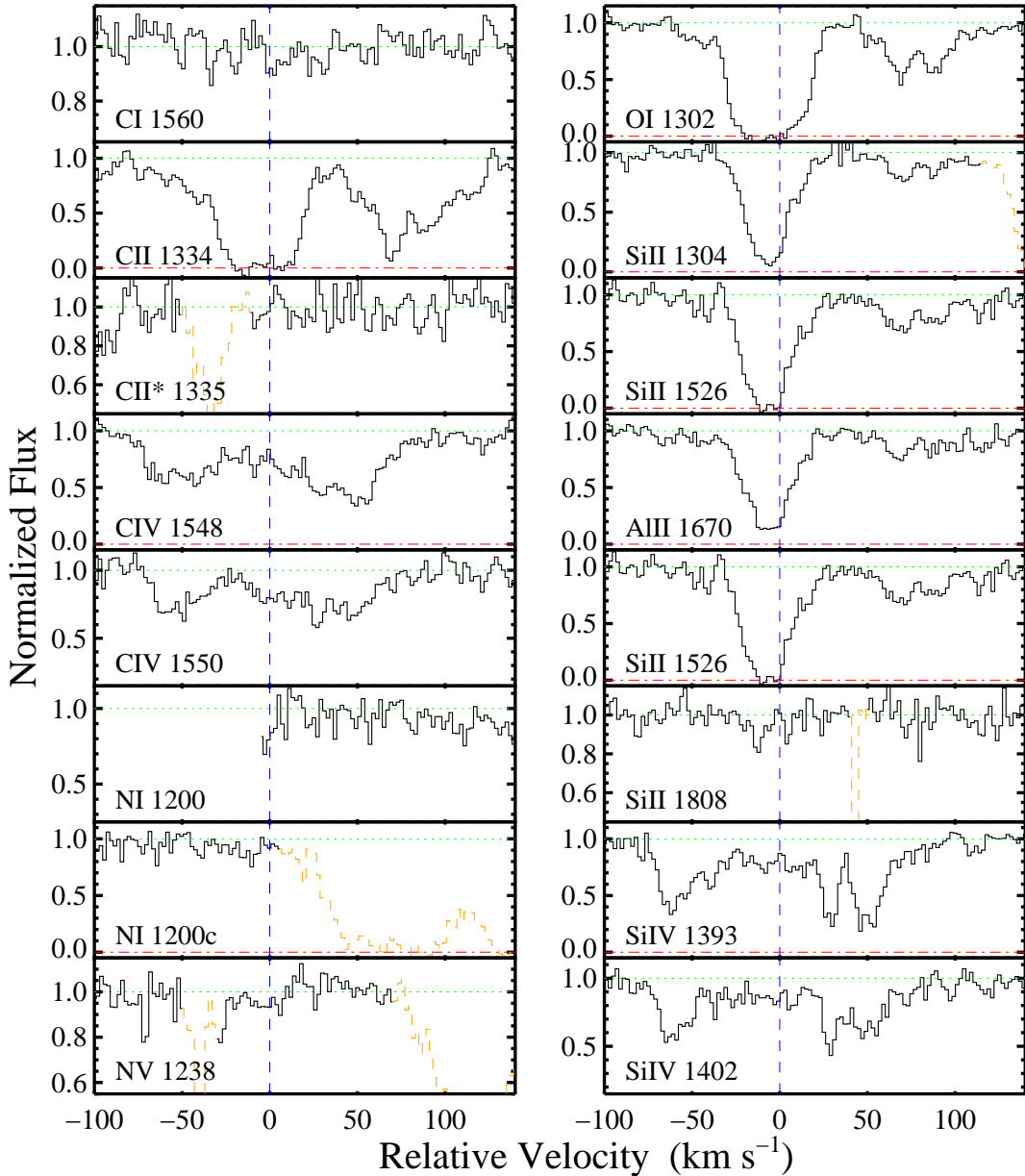
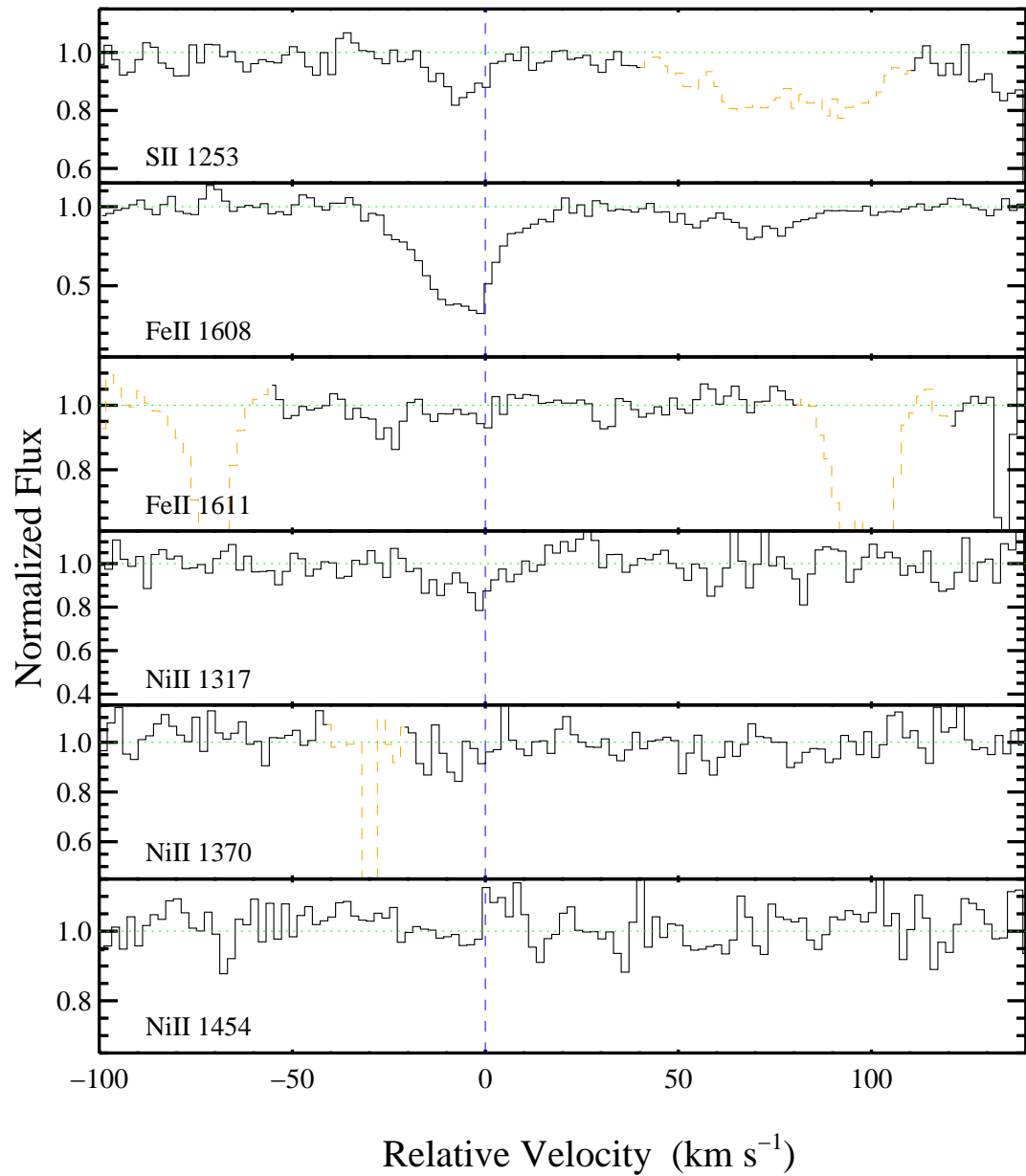


Fig. 5.— HIRES velocity profiles of the transitions identified with the damped Ly $\alpha$  systems at  $z = 2.9489$  toward Q1021+30.



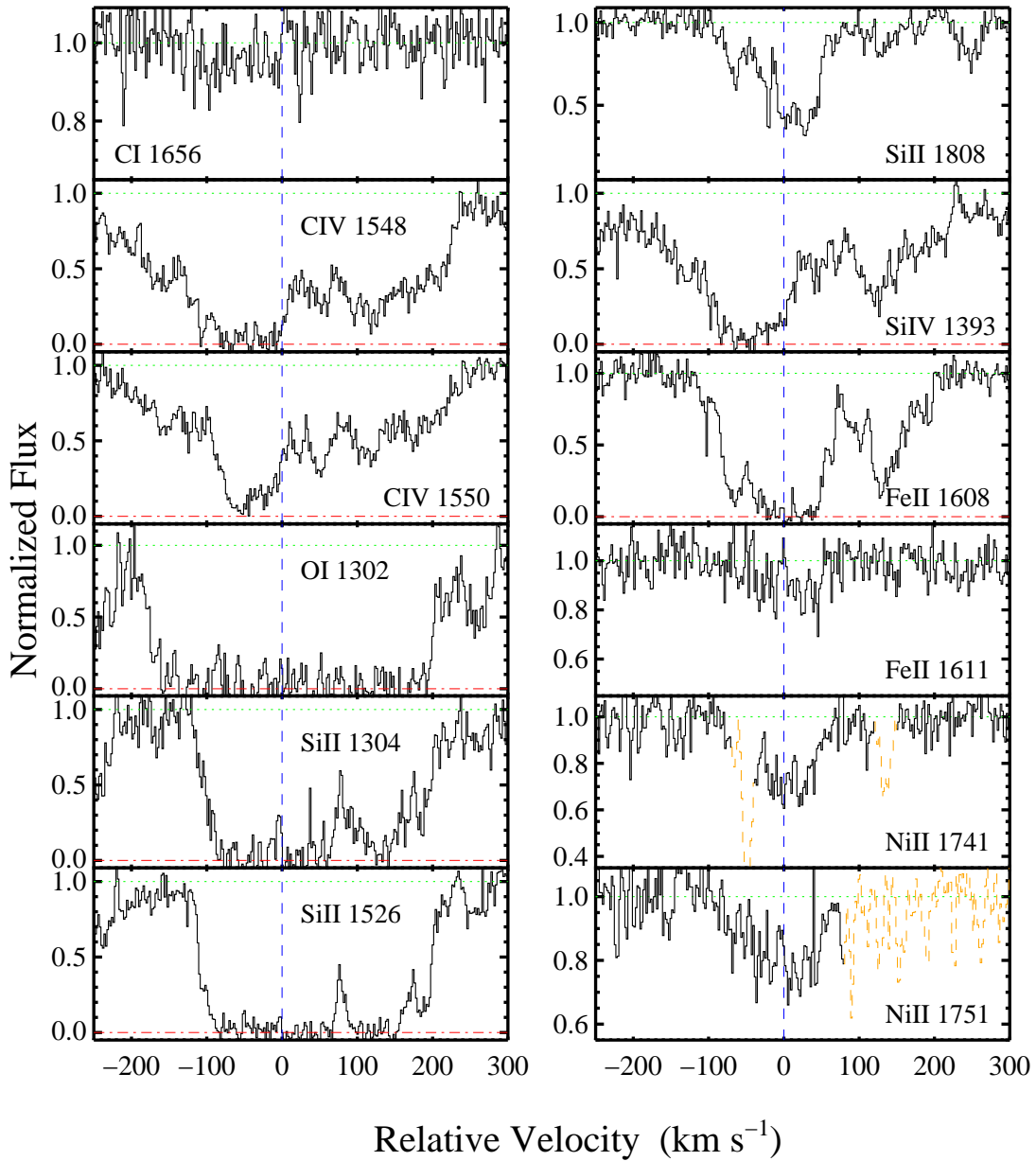


Fig. 6.— HIRES velocity profiles of the transitions identified with the damped Ly $\alpha$  systems at  $z = 2.5841$  toward Q1209+0919.

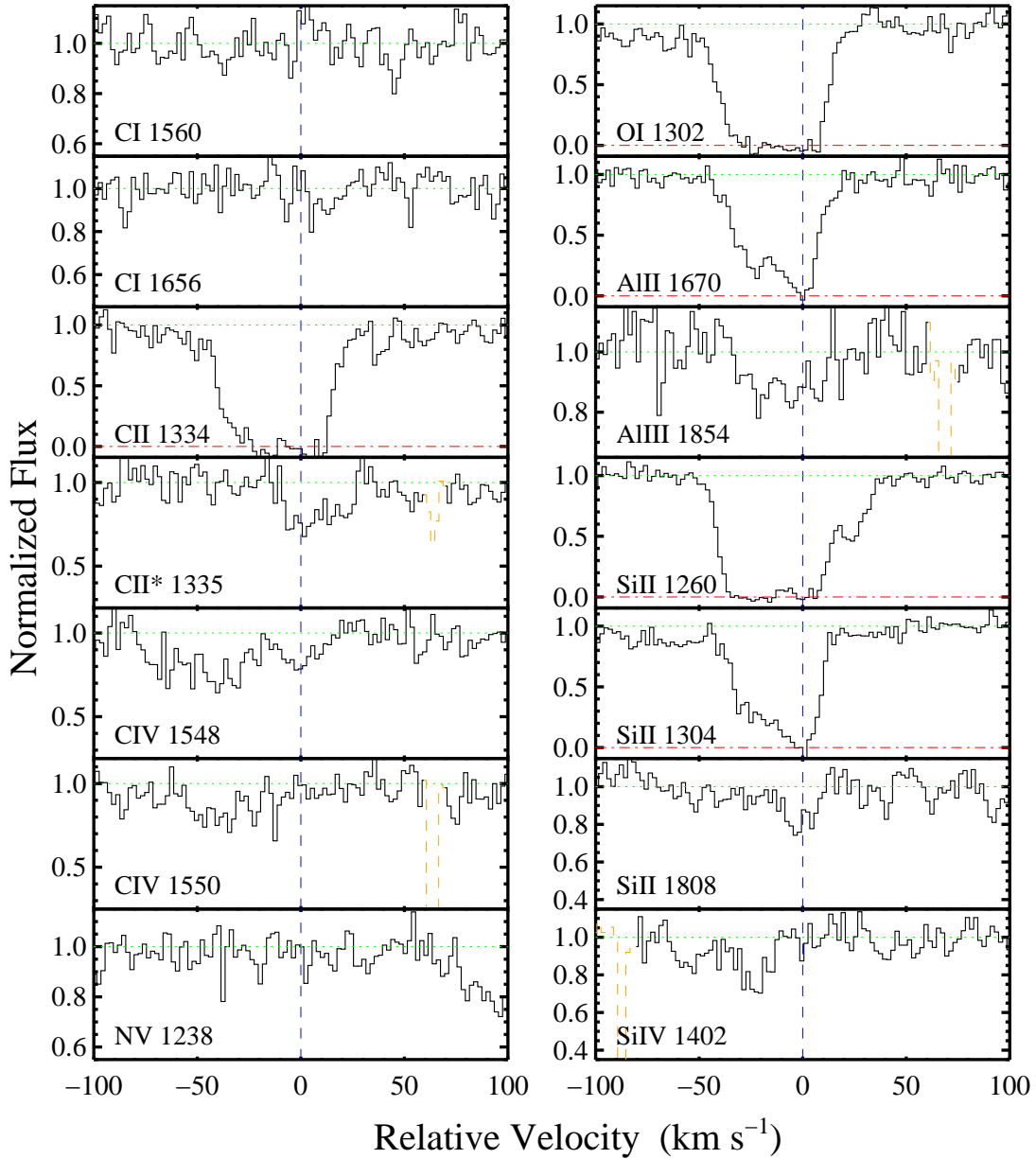
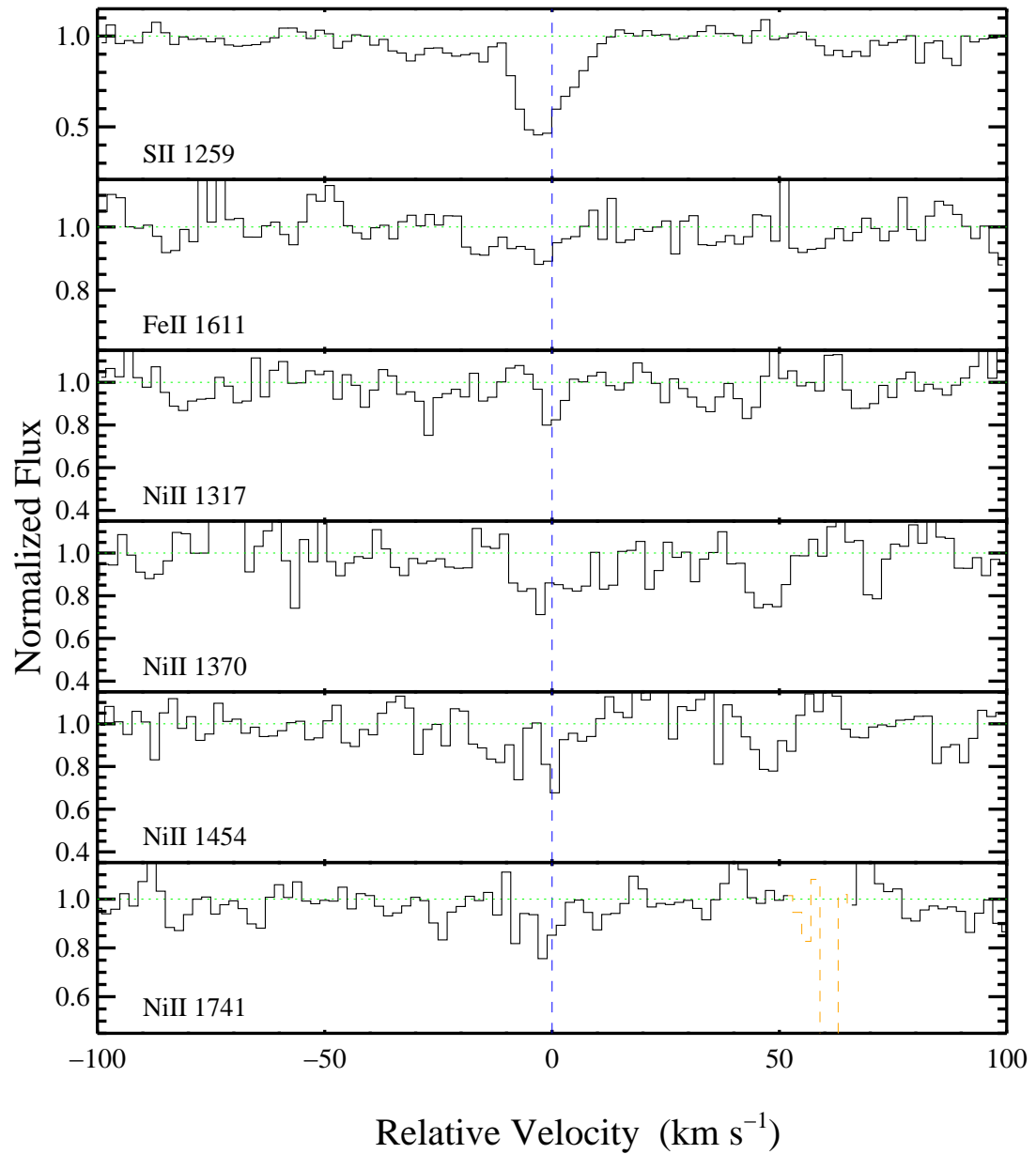


Fig. 7.— HIRES velocity profiles of the transitions identified with the damped Ly $\alpha$  systems at  $z = 2.79585$  toward Q1337+11.



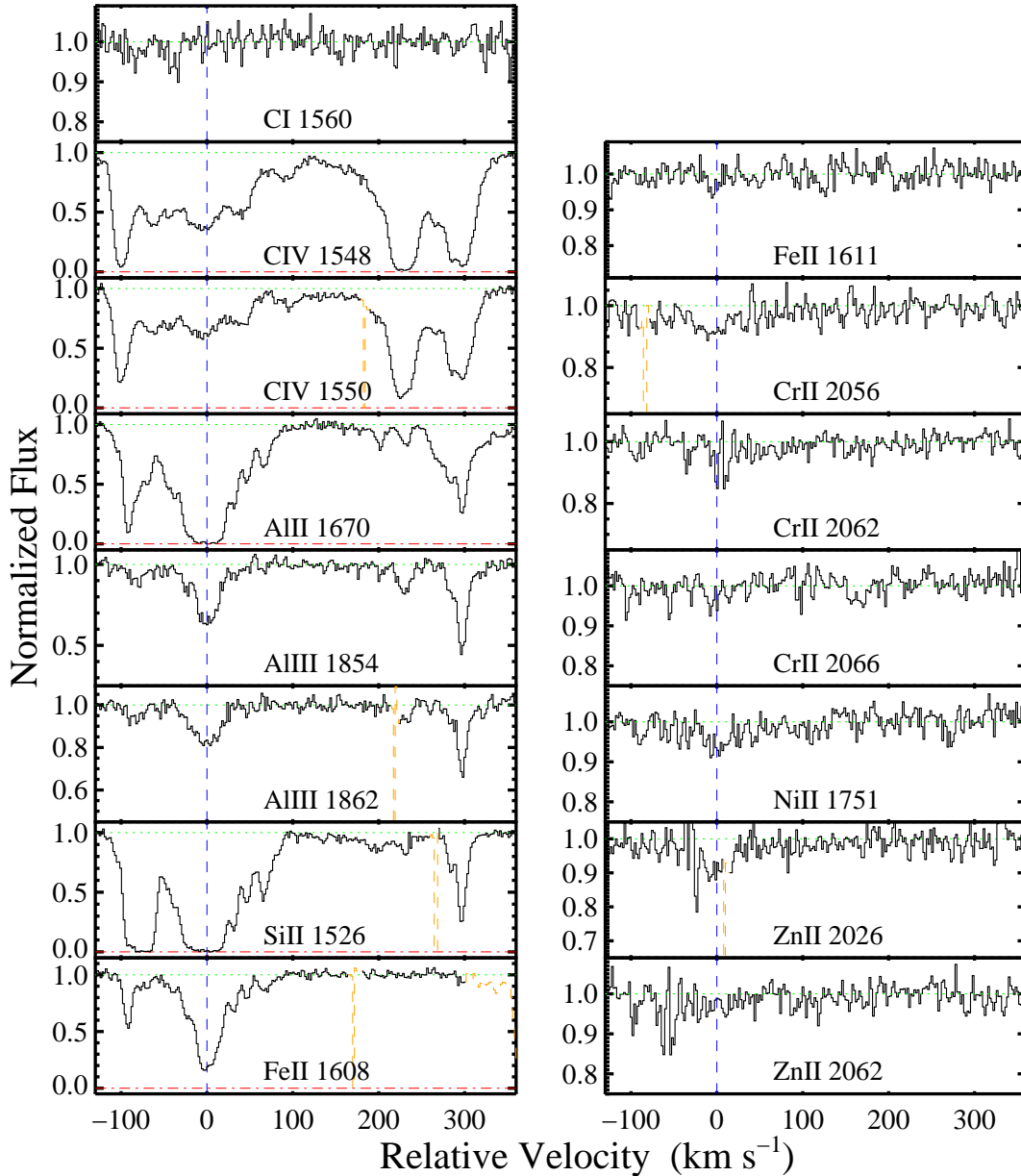


Fig. 8.— HIRES velocity profiles of the transitions identified with the damped Ly $\alpha$  systems at  $z = 2.8268$  toward Q1425+60.

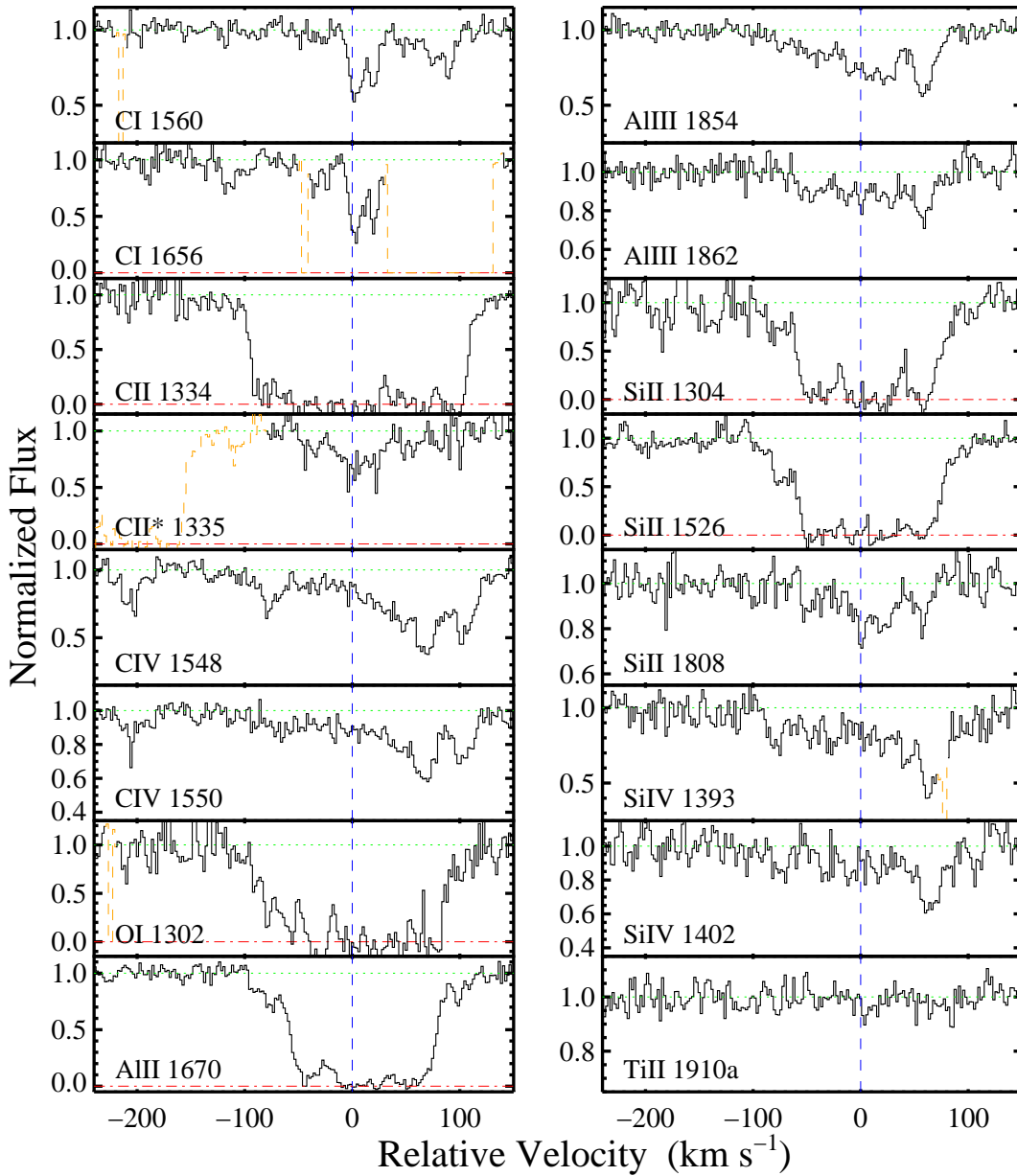
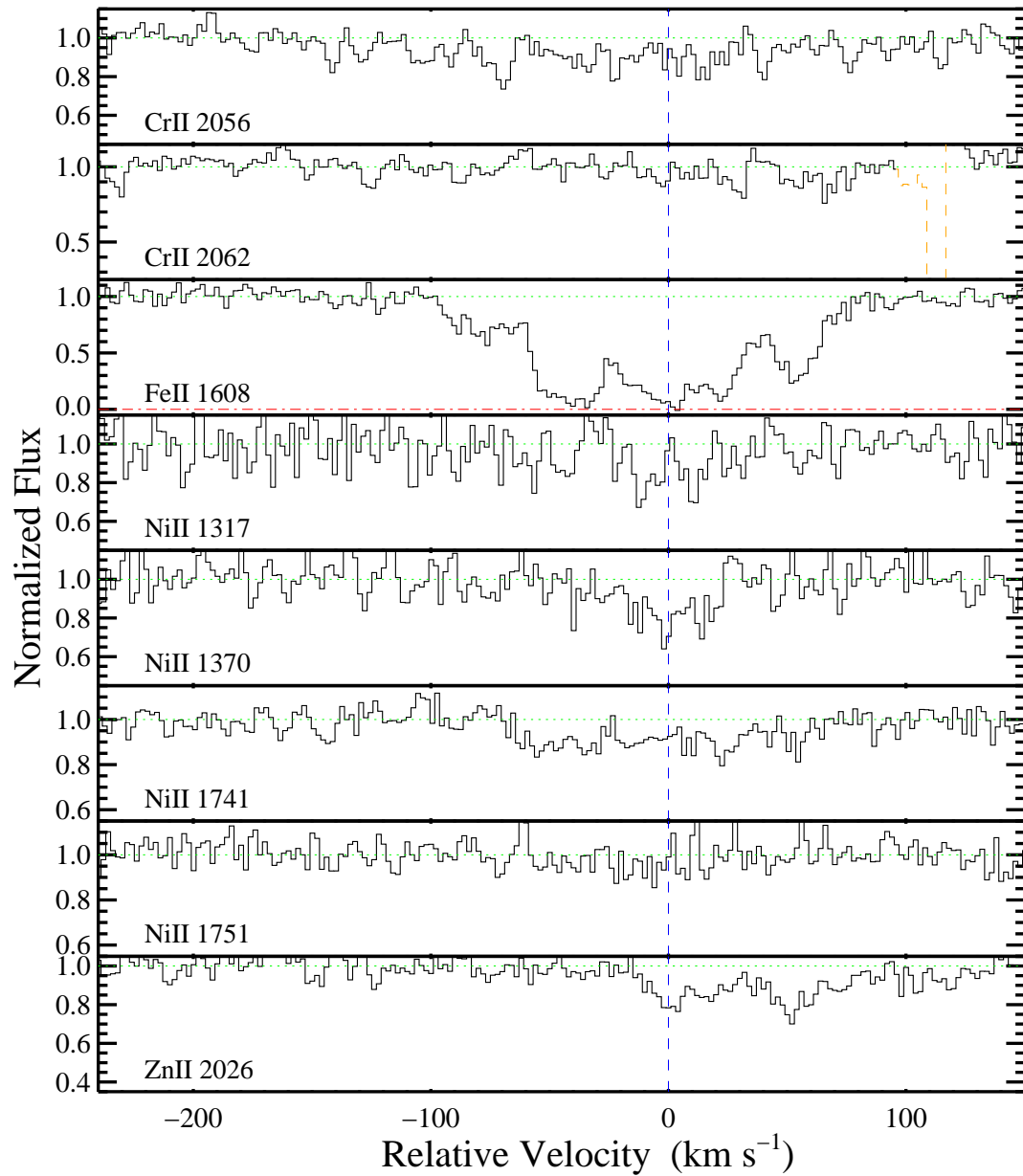


Fig. 9.— HIRES velocity profiles of the transitions identified with the damped Ly $\alpha$  systems at  $z = 2.05452$  toward J2340–00.



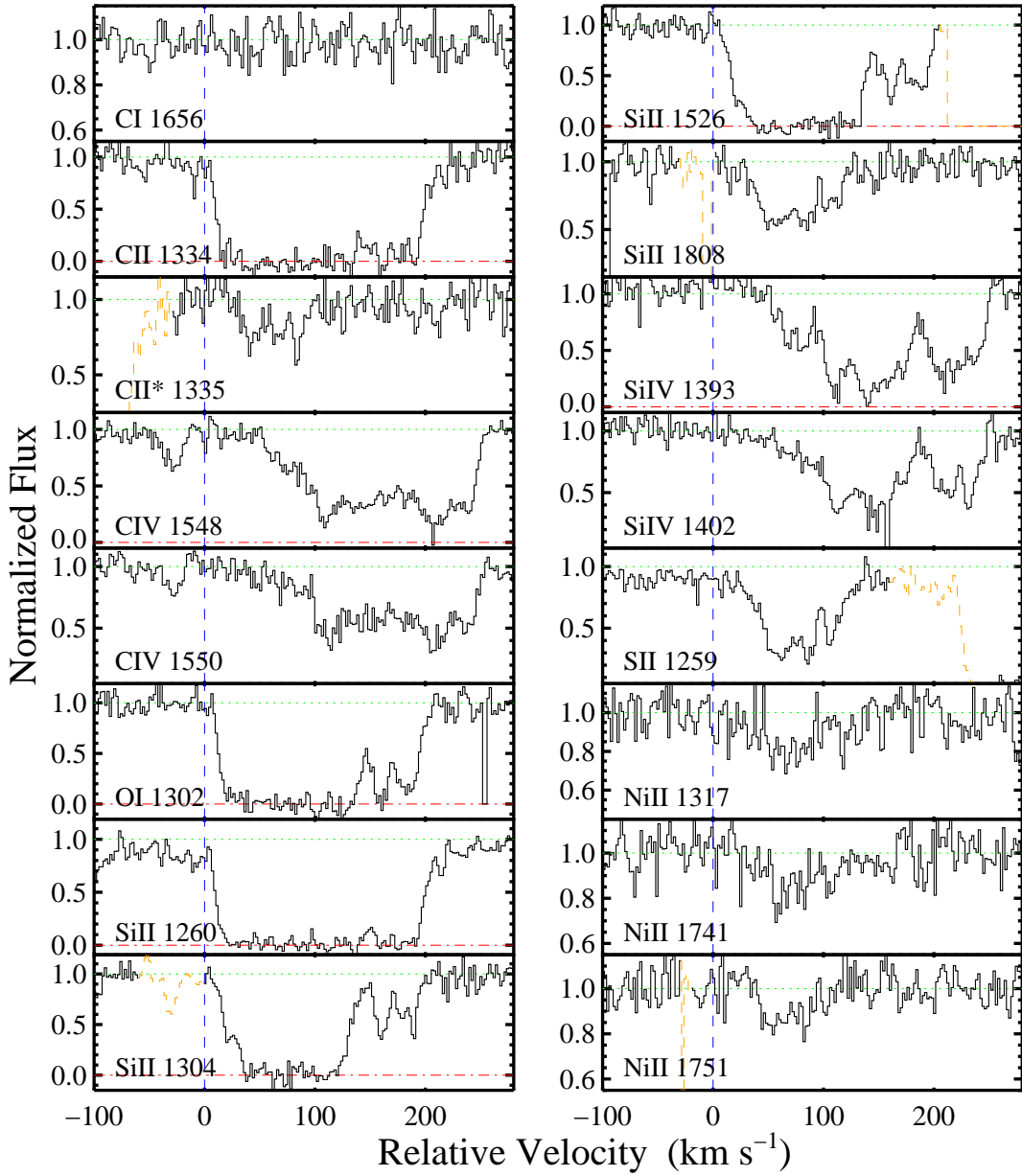


Fig. 10.— HIRES velocity profiles of the transitions identified with the damped Ly $\alpha$  systems at  $z = 2.90823$  toward Q2342+34.

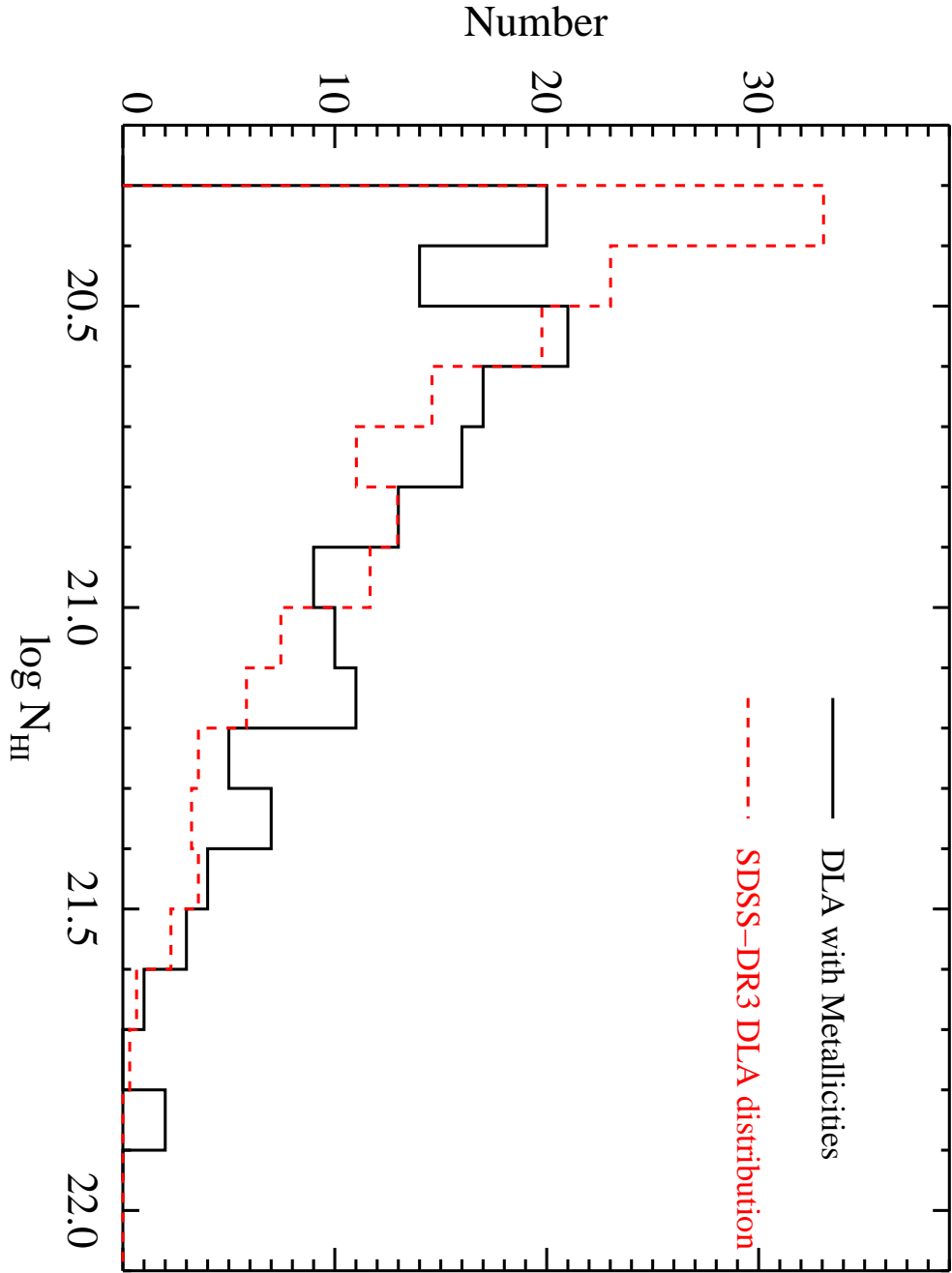


Fig. 11.—  $N_{\text{HI}}$  histogram for the damped Ly $\alpha$  systems comprising the  $z > 1.6$ , high-resolution sample of metallicity measurements (Table 13). Overplotted on the histogram is the expected  $N_{\text{HI}}$  distribution for a random set of damped Ly $\alpha$  systems with the same number as our metallicity sample. This curve was generated from the  $N_{\text{HI}}$  frequency distribution measured by Prochaska, Herbert-Fort & Wolfe (2005) from the Sloan Digital Sky Survey. A two-sided KS test rules out the null hypothesis that the two distributions are drawn from the same parent population at  $> 99\%$ c.l.